UMEÅ UNIVERSITY

Modelling and analyzing strong-field effects in quantum plasma

Haidar Al-Naseri

Department of Physics
Umeå University, Sweden 2023

ISBN: 978-91-8070-067-2(print) ISBN: 978-91-8070-068-9 (pdf)
Cover art by: Jens Zamanian
Electronic version available at: http://umu.diva-portal.org/
Printed by: CityPrint i Norr AB
Umeå, Sweden 2023

To my family

(This page is intentionally left blank)

Abstract

Under the extreme conditions that can be found around dense stars and in the accretion discs of black holes, several strong-field quantum phenomena dominate the dynamics of the plasma. This includes the creation of matter and anti-matter from the vacuum (Schwinger mechanism), radiation reaction and Landau quantization. Some of these strong field phenomena were presented theoretically a century ago but have never been verified in experiments due to the difficulty of creating the required extreme conditions in the lab. However, with the development of laser facilities in the past decades, it will be possible to observe several extreme physical phenomena in the near future. To conduct experiments on these extreme phenomena, theoretical simulations need to be constructed as a guide for optimizing experiments.

This thesis is concerned with developing and analyzing strong field phenomena in kinetic plasma models. The focus is to extend current kinetic models to include several physical phenomena that are relevant to future experiments on laser-plasma interaction. In particular, a kinetic theory based on the Wigner transformation of the Dirac equation has been analyzed in different regimes. This kinetic model is used to study the plasma dynamics at the Schwinger limit, where collective plasma effects and several quantum processes are studied.

Publications

This thesis is based on the following publications:

I **Relativistic kinetic theory for spin-1/2 particles: Conservation laws, thermodynamics, and linear waves**
R. Ekman, H. Al-Naseri, J. Zamanian, G. Brodin
Phys. Rev. E **100**, 023201 (2019).

II **Kinetic theory for spin-1/2 particles in ultrastrong magnetic fields**
H. Al-Naseri, J. Zamanian, R. Ekman, G. Brodin
Phys. Rev. E **102**, 043203 (2020).

III **Plasma dynamics and vacuum pair creation using the Dirac-Heisenberg-Wigner formalism**
H. Al-Naseri, J. Zamanian, G. Brodin
Phys. Rev. E **104**, 015207 (2021).

IV **Linear pair-creation damping of high-frequency plasma oscillation**
H. Al-Naseri, G. Brodin
Phys. Plasmas **29**, 042106 (2022).

V **Radiation reaction effects in relativistic plasmas–the electrostatic limit**
H. Al-Naseri, G. Brodin
Phys. Rev. E **107**, 035203 (2023).

VI **Plasma dynamics at the Schwinger limit and beyond**
G. Brodin, H. Al-Naseri, J. Zamanian, G. Torgrimsson, B. Eliasson
Phys. Rev. E **107**, 035204 (2023).

VII **Applicability of the Klein-Gordon equation for pair production in vacuum and plasma**
H. Al-Naseri, G. Brodin
To be submitted.

Other publications by the author that are not included in the thesis:

- **Short-scale quantum kinetic theory including spin–orbit interactions**
  R. Ekman, H. Al-Naseri, J. Zamanian, G. Brodin
  Eur. Phys. J. D **75**, 1-13 (2021).

- **Ponderomotive force due to the intrinsic spin for electrostatic waves in a magnetized plasma**
  H. Al-Naseri, G. Brodin
  arXiv:2302.05136. Submitted to *Phys. Plasmas*

Contents

Chapter 1

Introduction

An essential part of physics is making experiments that aim in verifying theoretical predictions. The information from the experiments tests whether the predictions from theory are correct or not. However, since experiments include many parameters and often complex interactions, it can be hard to interpret the output data. Thus, theoretical models of experiments are necessary to construct in order to illustrate the complex interactions that happen during the experiments. These models describe the different theoretically predicted processes that often happen in a very short time. The data from the theoretical models is benchmarked with the output data from experiments. By doing so, one can strengthen the validity of theoretical predictions, and if the predictions are invalid, new theories need to be constructed.

In the past decades, the interest for conducting experiments on strong field effects in plasma has increased [1]. This has been motivated by the steady increase in the technological development of laser facilities [2–4] . This opened the door for conducting experiments that would access new regimes of physics [5, 6]. In particular, the combination of high-energy particle beams and high intensity laser fields will access the nonlinear and relativistic quantum plasma regimes. To conduct experiments in this regime, theoretical models of relativistic plasma that interact with strong lasers need to be developed [7–11].

This thesis is about the theoretical modelling of strong field effects in plasma. In this thesis, kinetic equations that describe the interaction of dense plasma with external electromagnetic fields are developed and

analyzed. These kinetic equations model the dynamics of plasma that can be found in laser-plasma experiments or in astrophysical environments [12]. The theoretical models used in this thesis can also be used to study other quantum effects related to high-density plasma. For certain classes of plasmas where the density is very high, several quantum effects become important. These high-density plasmas can also create strong fields from which electron-positron pairs can be created. This has also been a part of this thesis. To be more concrete about which strong field effects we are interested in, this chapter will briefly describe the ones we are studying in this thesis.

1.1 Pair production

Electron-positron pairs can be created from vacuum by strong electric fields, also known as the Schwinger mechanism. How strong an electric field E should be to create pairs from vacuum through this mechanism can be characterized by the critical field E_{cr}

$$E_{cr} = \frac{m^2 c^3}{q\hbar} \tag{1.1}$$

where m and q are the mass and charge of the produced particles, $\hbar$ is the reduced Planck constant and c is the speed of light. For the case of electron charges, one has the critical field $E_{cr} = 1.32 \times 10^{18} V/m$. The Schwinger mechanism was first proposed by Sauter in 1931 [13]. However, a complete mathematical description of this phenomenon was constructed by Julian Schwinger in 1951 [14]. What Julian Schwinger found was that the rate Γ to create an electron-positron pair from vacuum per unit volume is

$$\Gamma = \frac{c^5 m_e^4 E^2}{4\pi^3 \hbar^4 E_{cr}^2} \exp\left\{-\pi \frac{E_{cr}}{E}\right\} \tag{1.2}$$

where m_e is the mass of electron. From this equation, one can conclude that the probability for the Schwinger mechanism is heavily suppressed for fields that satisfy the condition $E \ll E_{cr}$. This explains why the Schwinger mechanism has not been observed yet, as it has not been possible to create fields of the order of E_{cr} in experiments. However, due to the development of laser technology in the past decades, the interest in conducting experiments on the Schwinger mechanism has increased. Hence, many works have been devoted to create theoretical models of future experiments on the Schwinger mechanisms [5, 15–17].

There are also other mechanisms that enable the production of electron-positron pairs besides the Schwinger mechanism. By letting two photons collide, one can produce an electron-positron pair, also known as the Breit-Wheeler process [18].

$$\gamma + \gamma \rightarrow e^+ + e^- \tag{1.3}$$

where γ and $e^{\pm}$ represent photon and positron/electron. If we have a system with many photons, let us say a high-energy photon γ that propagate in an electromagnetic field with n photons, we get

$$\gamma + n\hbar\omega \rightarrow e^+ + e^- \tag{1.4}$$

This process is called nonlinear Breit-Wheeler, where $\hbar\omega$ is energy from one photon of the electromagnetic field. The electromagnetic field in this context is often a laser field with a large number of coherent photons. This makes it possible to consider the laser field as a classical, non-quantized field. The nonlinear Breit-Wheeler process has been observed in an experiment at SLAC in 1997 [19] where a high-energy electron beam collided with a counter-propogating laser pulse.

It is also possible to create an electron-positron pair from only a classical electromagnetic field. Although the electromagnetic field is treated classically, due to the wave particle interaction, a single quanta is absorbed from the electromagnetic field to produce an electron-positron pair

$$\hbar\omega \rightarrow e^+ + e^- \tag{1.5}$$

This process can be described using a mean-field formalism where each quanta is interacting with a big number of particles, in this context virtual particles, for more details see Paper IV The single quanta process requires that each quanta of the classical electromagnetic field carry the energy

$$\hbar\omega \geq 2m_e c^2 \tag{1.6}$$

More than a single quanta can also be absorbed to create an electron-positron pair, and this would soften the condition in Eq. (1.6), for more details, see Ref. [17]. The considerations made in this section are relevant for Paper III, IV, and VI.

1.2 Radiation reaction

A plasma consists of a large number of charged particles that experience different forces when interacting with an external electromagnetic field. Thus,

in the laser-plasma interaction, the motion of the plasma is changed due to the different forces it experiences. As is well known, an accelerating charged particle emits electromagnetic radiation and loses energy. This loss of energy causes a recoil force on the emitting particle known as the *radiation reaction*. By that, the collective dynamics of the charged particles in the plasma is affected by the single particle radiation reaction when the plasma is interacting with external electromagnetic fields. The physics of the radiation reactions has been known in classical electrodynamics [20–23] for more than a century. While the fundamentals of classical radiation reactions have been known for a long time, the consequences for collective plasma dynamics have not been explored until recently.

For plasma and electromagnetic field interactions that occur at very short time intervals and on small length scales, classical models of radiation reactions break down [24]. For these processes, a quantum mechanical description of the radiation reaction is needed. Charged particles emit discrete photons, not continues emission as in the classical picture. This affect the radiation reaction force and hence the dynamics of the emitting particles [25–27]. Experiments that observed quantum radiation reaction has done recently [28]. The radiation reaction force has been considered in Paper V.

1.3 Other strong-field effects

In the ultrastrong magnetic field of magnetars [12] and in intense laser-plasma interactions [29], there are several quantum effects that become important. These effects are related to spin dynamics and are covered in this thesis. There are also other strong-field effects that arise due to vacuum polarization.

Landau-quantization: In a very strong and slowly varying magnetic field, charged particles can only occupy discrete states of the cyclotron orbits. This affects the motion of the charged particles, as they can only be found in discrete cyclotron orbits with equidistant energy levels. This effect is known as the *Landau quantization*. Such a magnetic field can be found in dense stars [12]. The effects due to strong magnetic fields on the dynamics of the plasma have been studied in Paper II.

Vacuum polarization: In quantum mechanics, the vacuum consists of virtual particles that polarize the vacuum in the same way as a dielectric medium does. This affects the measurement of different processes. Further-

more, several processes arise due to the vacuum polarization. This includes the light-light interaction [30, 31] and the one photon splitting due to strong magnetic fields [32]. Recently, there has been an observation of the light-light scattering at the ATLAS experiment at CERN [33].

1.4 Outline

I begin the thesis by considering the classical properties of plasma. These classical properties need to be considered in the laser-plasma interaction even if quantum models are to be used. In Section 2.1, I present the basic plasma parameters that characterize the collective physics of a plasma. In Section 2.2, the equations of motion of the collective plasma dynamics are presented. The linear response of plasma to external fields is discussed in Section 2.3. Finally, the wave particle interaction is discussed in Section 2.4 with a focus on the linear wave damping, also known as the *Landau-damping*.

While classical plasma models work well at modest temperatures and densities, quantum effects become important at low temperatures and/or high densities. Thus, in Chapter 3, the kinetic plasma models are extended to include several quantum effects. In Section 3.2, a transformation that enables the classical interpretation of quantum formulations is introduced. This transformation is used to derive kinetic theories of plasma, including quantum effects. To derive these kinetic theories, a transformation of the Dirac Hamiltonian that decouple the particle and antiparticle states is presented in Section 3.3. Finally, in Section 3.4, a quantum kinetic theory of spin-1/2 particles in ultrastrong magnetic fields is presented.

In very strong electromagnetic fields, the creation of electrons and positrons from vacuum is not negligible. In Chapter 4, kinetic models that include the pair creation physics in the dynamics of the plasma are studied. In Section 4.1, a kinetic equation that is based on the Wigner transformation of the Dirac equation, so-called Dirac-Heisenberg-Wigner (DHW) formalism, is presented. In particular, a simplified model in the electrostatic limit of this kinetic equation is presented. Then, a linear study of the DHW-formalism is presented in Section 4.2. Here, a pair creation damping mechanism similar to the linear Landau-damping is derived. To study nonlinear effects using the DHW-formalism, a numerical solution in the electrostatic limit is presented in Section 4.3. Here, the focus is to determine how the Schwinger mechanism affects the different collective plasma effects. Finally, an alternative formalism to the DHW-formalism, so-called Klein-Gordon-Wigner (KGW) formalism, is presented in Section 4.4. Here

the model is based on a Wigner transformation of the Klein-Gordon equation instead of Dirac. This model can be used to represent fermions under certain conditions, and these conditions are discussed in Section 4.4.

Finally, in Chapter 5 the effect of radiation has been added to the dynamics of the plasma. In Section 5.1, the classical radiation reaction is introduced. Then, in Section 5.2, the effects of the radiation reaction have been added to the relativistic Vlasov equation. The consequence of this extension has been analyzed, and a cooling mechanism in the background plasma due to the radiation reaction has been found.

Chapter 2

Classical plasma physics

Plasma is the most common state of visible matter in the universe and can be found in stars, solar winds, planetary magnetospheres, and the interstellar medium. One can also find plasma in science laboratories and in the fabrication of semiconductors. Plasma is perhaps most known for being used to obtain clean energy in future fusion energy reactors [34]. There has been a large investment to produce clean energy by confining hot and dense plasma for sufficiently long times to obtain a fusion of deuterium nuclei into helium nucleus [35].

What characterizes the plasma is that it is overall electrically neutral but contains charge carriers that can move freely. In this chapter, a short introduction to classical plasma properties is given. In the first section, basic plasma parameters are presented. Following that, in Section 2.2 two methods for modelling plasma dynamics will be presented. Then, linear plasma responses to external fields will be described in Section 2.3. Finally, wave-particle exchange effects are discussed in Section 2.4 with a focus on the linear Landau damping.

2.1 Basic plasma physics

A plasma is an ionized gas in which the typical kinetic energies of the particles are much greater than the potential energy in relation to its nearest neighbor [36]. Thus, by heating a neutral gas, the electrons will separate from the atoms, and we gradually obtain a gas of electrons and ions, i.e., plasma. The plasma is composed of free charges, it is highly conductive, and any charge

imbalance is quickly neutralized by the free-moving charge carriers in the plasma. If a test charge is introduced into the plasma, the test charge's field will affect the plasma's surrounding particles. The response from the plasma is that it will surround the test charge with a cloud of particles of the opposite charge, which screens the test charge. This effect is called *Deby screening* and is dependent on the plasma parameters: temperature T, charge q, and number density n [34, 37]. The characteristic length of the screening λ_D from the plasma on the test charge q_t is called *Deby length* and is defined as

$$\lambda_D = \sqrt{\frac{k_B T}{4\pi n q^2}} \tag{2.1}$$

where k_B is the Boltzmann constant. The number of particles inside a cube with length λ_D is called the *plasma parameter*.

For an ion-electron plasma, the particles can generate and respond to electromagnetic fields. However, ions are much heavier than electrons; a proton weighs about ~ 2000 more than an electron. This makes the electrons more mobile, and unless the considered waves are of low frequencies, the ions are slow to respond to the propagation of waves and neutralize them. Thus, in the case of high frequencies, the ions can be regarded as a neutralizing background for the electrons, and only the electron dynamics are considered. If we assume that we have a neutralized plasma and displace some of the electrons, the charge separation will create an electric field. This field will force the electrons back to their original positions to restore neutrality. However, the accelerated electrons will pass their original positions due to inertia and end up with a charge imbalance. This will continue back and forth, creating an oscillating system with a frequency ω_p called *plasma frequency* defined as

$$\omega_p = \sqrt{\frac{4\pi q_e^2 n_e}{m_e}} \tag{2.2}$$

where q_e, n_e and m_e are the charge, density, and mass of the electron, respectively.

2.2 Plasma description

To completely determine the state of a plasma, one needs to know the velocity and position of all particles. However, since a plasma contains a large number of particles, this is an impossible task, and hence one needs to use a statistical

approach to determine the state of the plasma. There are two main ways to model a plasma, kinetic and fluid descriptions.

2.2.1 Kinetic description

The classical state of a plasma is described in kinetic theory by the distribution function $f_s(\mathbf{r}, \mathbf{p}, t)$ representing the phase space number of particles of species s (electrons or ions) at position $\mathbf{r}$ with the momentum $\mathbf{p}$ at time t. The number particle density $n_s(\mathbf{r}, t)$ is obtained from

$$n_s(\mathbf{r}, t) = \int d^3p f_s(\mathbf{r}, \mathbf{p}, t) \tag{2.3}$$

A plasma interacts with an external electromagnetic field, where the evolution of the distribution function $f_s(\mathbf{r}, \mathbf{p}, t)$ was firstly derived by Vlasov [38]

$$\partial_t f_s(\mathbf{r}, \mathbf{p}, t) + \frac{\mathbf{p}}{m_s} \cdot \nabla_r f_s(\mathbf{r}, \mathbf{p}, t) + q_s \left(\mathbf{E} + \frac{\mathbf{p}}{m_s c} \times \mathbf{B} \right) \cdot \nabla_p f_s(\mathbf{r}, \mathbf{p}, t) = 0 \tag{2.4}$$

where $\mathbf{E}$ and $\mathbf{B}$ are the electric and magnetic fields, respectively. The plasma responds to the propagation of an external field and creates its own fields. This is included self-consistently in the dynamics using Maxwell's equations

$$\begin{aligned} \nabla_r \cdot \mathbf{E} &= 4\pi\rho \\ \nabla_r \cdot \mathbf{B} &= 0 \\ \nabla_r \times \mathbf{E} &= -\partial_t \mathbf{B} \\ \nabla_r \times \mathbf{B} &= \frac{4\pi}{c}\mathbf{J} + \frac{1}{c}\partial_t \mathbf{E} \end{aligned} \tag{2.5}$$

where ρ and $\mathbf{J}$ are the charge and current density, respectively

$$\rho = \sum_s q_s \int d^3p f_s(\mathbf{r}, \mathbf{p}, t) \tag{2.6}$$

$$\mathbf{J} = \sum_s q_s \int d^3p \frac{\mathbf{p}}{m_s} f_s(\mathbf{r}, \mathbf{p}, t) \tag{2.7}$$

where a summation of the species s has been used. The Vlasov equation is one of the most important plasma equations and can be used to model a large number of systems in plasma physics. The Vlasov equation can be used to study linear waves, in particular cyclotron and Landau-damping [39].

Moreover, Eq. (2.4) capture strongly nonlinear motion very well. However, Eq. (2.4) is non-relativistic, a relativistic version of Eq. (2.4) is presented in Section 5.2. The relativistic Vlasov equation can be used to model the case of fully relativistic electron motion due to a strong laser field.

2.2.2 Fluid description

In cases of inhomogeneous media, complex magnetic field structures or other complications, a kinetic description of seven independent variables may be too challenging, in which case a simpler description might be preferable. For this purpose, the fluid model can be used to model the dynamics of the plasma. The equations of the fluid model are obtained by integrating over various moments of the Vlasov equation Eq. (2.4). By doing so, the six-dimensional phase space is replaced with a three-dimensional one. The fluid equations are easier to solve numerically since we have only three independent variables in addition to time. However, phenomena such as wave-particle interaction and so-called finite Larmor radius effects (e.g., Bernstein resonances [40]) are excluded in the fluid description. Integrating the Vlasov equation Eq. (2.4) over momentum space, we get the continuity equation

$$\partial_t n_s(\mathbf{r},t) + \nabla_r \cdot \Big(n_s(\mathbf{r},t) \frac{\mathbf{p}_s}{m_s} \Big) = 0 \tag{2.8}$$

with $n_s(\mathbf{r},t)$ representing the number density. Next, we can multiply Eq. (2.4) by $\mathbf{p}$ and integrate over the momentum space to obtain the momentum equation

$$\partial_t p_{si}(\mathbf{r},t) + \Big(\frac{\mathbf{p}_s}{m_s} \cdot \nabla_r \Big) p_{si}(\mathbf{r},t) = q_s \Big(E_i + \varepsilon_{ijk} \frac{p_{sj}}{m_s c} \times B_k \Big) - \frac{1}{n} \frac{\partial P_{ij}}{\partial r_j} \tag{2.9}$$

where the summation of the repeated indices is assumed and ε_{ijk} is the Levi-Civita pseudotensor. This equation describes the effect of the total force on the fluid, where P_{ij} is the pressure tensor. The evolution equation of the pressure tensor P_{ij} is more complicated and involves the gradient of the heat tensor Q_{ijk} [41]. Eqs. (2.8) and (2.9) are coupled to Maxwell's equation Eq. (2.5) with the charge and current density given by

$$\rho(\mathbf{r},t) = \sum_s q_s n_s(\mathbf{r},t) \tag{2.10}$$

$$\mathbf{J}(\mathbf{r},t) = \sum_s \frac{q_s}{m_s} n_s(\mathbf{r},t) \mathbf{p}_s(\mathbf{r},t) \tag{2.11}$$

The fluid equations, including the evolution of the pressure tensor, can be closed by some suitable assumptions. One assumption is that the heat tensor $Q_{ijk} = 0$, which makes the fluid equation together with the evolution of the pressure tensor self-consistent.

While kinetic models are the main focus of the thesis, it can be noted that fluid models play an important role in plasma physics. The fluid description can be good to use in some cases where kinetic deception is rather complicated. However, since the momentum dependence of the density function is lost, wave-particle effects such as Landau damping are not included.

2.3 Linear theory and plasma waves

A plasma consists of a large number of charged particles where the collective effects are dominant. This allows for a large number of wave modes to propagate in the plasma. To characterize these modes, a common physical approach is used, where one assumes that the response of the plasma to the waves is small compared to the plasma's static equilibrium state. Such an approach is known as the linear theory and is used for cases where the amplitude of the waves is small. Generally, ions are much heavier than electrons, and for waves with high frequencies, their dynamical motion can be neglected. Thus, we can neglect the response of ions to the waves and only consider the response of electrons. By that, we drop the subscript s in the following and use the electron charge $q_e = -e$. We can pick an example of the linear theory where we linearize the number density in phase space $f(\mathbf{r}, \mathbf{p}, t)$ as

$$f(\mathbf{r}, \mathbf{p}, t) = f_0(\mathbf{p}) + f_1(\mathbf{r}, \mathbf{p}, t) \tag{2.12}$$

where $f_0(\mathbf{p})$ is the constant number density of the equilibrium plasma, i.e., before the propagation of the waves in the plasma, and $f_1(\mathbf{r}, \mathbf{p}, t)$ is the perturbed number density due to the propagation of waves. A similar division of perturbed and unperturbed quantities is done for the electromagnetic field as well. The requirement for this approach to be valid is $f_1(\mathbf{r}, \mathbf{p}, t) \ll f_0(\mathbf{p})$ and that we have electromagnetic fields with modest amplitudes. This allows for an approximation in which the product of perturbed quantities and higher-order terms is neglected. Looking at the third term of Eq. (2.4), we notice that

$$\mathbf{E} \cdot \nabla_p f = \mathbf{E}_1 \cdot \nabla_p (f_0 + f_1)$$

Here, $E_1 f_1$ can be ignored, and we only keep $E_1 f_0$. For simplicity, we can now consider the case where the magnetic field is vanishing and we have electrostatic waves in the plasma. Then Eq. (2.4) is reduced to

$$\partial_t f_1 + \frac{p_z}{m}\partial_z f_1 - eE_1(z,t)\partial_{p_z} f_0 \tag{2.13}$$

and Ampere's law is linearized to

$$\partial_t E_1 = -4\pi \frac{e}{m}\int d^3p\, p_z f_1 \tag{2.14}$$

Next, we can use the wave-plane ansatz

$$f_1(\mathbf{r},\mathbf{p},t) = \tilde{f}_1(\mathbf{p})e^{i(\mathbf{k}\cdot\mathbf{r}-\omega t)} \tag{2.15}$$

where $\tilde{f}_1(\mathbf{p})$ is the amplitude of f_1 in momentum space and $\mathbf{k}$ and ω are the wave vector and frequency of the wave, respectively. Using this ansatz in Eqs. (2.13) and (2.14), we get

$$f_1 = i\frac{eE_1}{(\omega - kp_z/m)}\partial_{p_z} f_0 \tag{2.16}$$

$$E_1 = -i4\pi \frac{e}{m\omega}\int d^3p\, p_z f_1 \tag{2.17}$$

Using the expression of f_1 in the Ampere's law, we get the dispersion relation $D(\omega,k)=0$

$$D(\omega,k) = 1 + \frac{4\pi e^2}{\omega m}\int d^3p \frac{p_z}{\omega - kp_z/m}\partial_{p_z} f_0 = 0 \tag{2.18}$$

Considering the low-temperature limit where $kp_z/m \ll \omega$ and keeping the lowest order non-vanishing term, we get after integration by parts

$$\omega^2 = \frac{4\pi e^2}{m}\int d^3p f_0 = \frac{4\pi e^2 n_0}{m} = \omega_p^2 \tag{2.19}$$

where in the last equality we have used the definition of plasma frequency. However, if we include up to first order in $kp_z/m\omega$ in Eq. (2.18), the dispersion relation becomes

$$D(\omega,k) = 1 - \frac{\omega_p^2}{\omega^2} - \frac{3k^2 p_{th}^2 \omega_p^2}{m^2\omega^4} = 0 \tag{2.20}$$

where we have defined the thermal momentum p_{th} as

$$p_{th}^2 = \frac{1}{n_0}\int d^3p\, p_z^2 f_0 \tag{2.21}$$

2.4 Landau-damping

The dispersion relation in Eq. (2.18) was firstly derived by Vlasov [38]. While Vlasov solved the dispersion relation using the principal value of the integral, Landau showed in [39] that this approach neglects an important effect. This effect is related to the singularity that occurs for $\omega = kp_z/m$. Landau suggested that the frequency ω must have an imaginary part: $\omega = \omega_r + i\omega_i$, where ω_r and ω_i are the real and imaginary frequencies, respectively. Assuming that: $\omega_i \ll \omega_r$, one can Taylor-expand the dispersion relation $D(\omega, k)$ to first order around ω_r:

$$0 = D_r(\omega_r, k) + iD_i(\omega_r, k) + i\omega_i \frac{\partial D_r}{\partial \omega} \mid_{(\omega_r, k)} \tag{2.22}$$

The integral in $D(\omega, k)$ Eq. (2.18) should be evaluated as a contour integral in the complex p_z-plane. The singularity in $D(\omega, k)$ is treated using the Plemelj formula

$$\frac{1}{u-a} = P\frac{1}{u-1} + i\pi\delta(u-a) \tag{2.23}$$

where P is the principal value employed by Vlasov in his approach and δ is the delta-function. Thus, all points in the p_z-coordinate are covered by the principal valued integral except the point at the singularity, which is included in the delta-function. Thus, the imaginary frequency ω_i is determined by solving both the real $D_r(\omega_r, k)$ and imaginary part $D_i(\omega_r, k)$. Considering the low-temperature limit of Eq. (2.20), we have the following expression of the real frequency ω_r

$$\omega_r^2 = \omega_p^2 + 3k^2 \frac{p_{th}^2}{m^2} \tag{2.24}$$

Using this expression of ω_r in Eq. (2.22) together with Eq. (2.18), we get

$$\omega_i = \frac{\pi\omega_p^3}{2k^2} f'\Big(\frac{p_z}{m} = \frac{\omega_r}{k}\Big) \tag{2.25}$$

This expression is valid in the limit $\omega_r/k \gg p_{th}/m$, indicating that the wave's phase velocity is much greater than the thermal velocity of electrons in the plasma. Thus, there is an exchange of energy between the electrons in the plasma and the external wave. This exchange causes a damping of the wave, called *Landau damping*. If the opposite were to hold, i.e., the electrons have a higher thermal velocity than the phase velocity, then the wave amplitude would grow and we would have an instability. One can summarize the physics

of Landau damping as follows: If particles move slower on average than the phase velocity of the wave with which they interact, they gain energy and the wave amplitude is damped. For the opposite case, particles that on average move faster than the phase velocity will lose energy, and the wave amplitude is increasing. Next, we use Eq. (2.22) to define the fraction γ.

$$\gamma \equiv \left| \frac{\omega_i}{\omega_r} \right| = \left| \frac{D_i(\omega_r, k)}{\omega_r(\partial D_r/\partial \omega_r)} \right| \tag{2.26}$$

This quantity can be used to estimate the importance of the Landau damping mechanism. Generally, the Landau damping mechanism is one of the most important theoretical predictions in plasma physics. This mechanism can only be modeled using kinetic theories. This is because the wave-particle interaction is related to the momentum distribution of the electrons, and such information is not provided by the fluid model. We will see in Section 4.2, a mathematically similar damping process to Landau-damping, but one with a different physical meaning.

Chapter 3

Quantum kinetic theory

In the previous chapter, we discussed different plasma parameters and showed how to model plasma using kinetic and fluid theories. These models are based on classical mechanics and work well for modest temperatures and densities. However, for low-temperature and/or high-density plasma, quantum effects become important [42, 43]. The interest for quantum plasma has increased due to different applications, including laser-plasma interaction [2, 44, 45], spintronic devices [46, 47] and plasmonic devices [48–50]. In this chapter, we will model and analyze quantum effects using kinetic plasma models. The formalism presented in this chapter is used to derive quantum kinetic theories that can be seen as a quantum extension to the Vlasov equation. We will start this chapter by presenting the conditions that make quantum mechanics necessary to describe the dynamics of the plasma. Then, in Section 3.2, a transformation that enables quantum mechanical systems to be treated with a formalism resembling classical ones is introduced. Then we will introduce the so-called Foldy-Wouthuysen transformation in Section 3.3. This transformation is used to separate particle- and antiparticle states of the Dirac Hamiltonian. We end this chapter by deriving a quantum kinetic theory of spin-1/2 particles in ultrastrong magnetic fields. To simplify the equations used in this chapter, we set $c = 1$.

3.1 Quantum plasma regimes

Before presenting the theoretical foundation of the quantum kinetic plasma models, we can go through the conditions for the quantum effect to be

important. The first quantum effect is due to the uncertainty principle, which implies that the wave function of a particle cannot be localized in both momentum and spatial space. Generally, for a particle momentum p, the characteristic spread in spatial space is given by the *de Broglie wavelength* $\lambda = \hbar/p$. The typical momentum of the particles in a plasma with temperature T is p_T. Thus, the typical spread of the wave function is the thermal de Broglie wavelength.

$$\lambda_{dB} = \frac{\hbar}{p_T}$$

For dense plasma, the wave functions of the different particles overlap each other, which makes it necessary to use quantum mechanics for describing the dynamics of the plasma. Such dense plasma can be characterized by the condition

$$n\lambda_{dB}^3 \geq 1 \tag{3.1}$$

where the number of particles inside the de Broglie box is equal to or greater than one. For such plasma, quantum mechanics is needed to describe the dynamics of the plasma.

Another quantum effect that is important for the dynamics of the plasma is the Pauli exclusion principle, which becomes important when the temperature of the plasma is similar to or lower than the Fermi temperature T_F

$$\frac{T_f}{T} \geq 1 \tag{3.2}$$

where

$$T_F = \frac{(3\pi^2 n)^{2/3}}{2mk_B\hbar^2} \tag{3.3}$$

However, one can show that $T/T_f \propto n\lambda_{dB}^3$ and hence the conditions Eqs. (3.1) and (3.3) are the same.

A third quantum effect is due to the intrinsic angular momentum of the electrons, also known as spin. The electrons are spin-1/2 particles and have a magnetic moment, also known as *Bohr magneton* μ_B

$$\mu_B = \frac{e\hbar}{2m} \tag{3.4}$$

Thus, electrons interact with external magnetic fields with interaction energy $\mu_B B$, where B is the magnitude of the external magnetic field. Comparing

this interaction energy with typical kinetic energy $k_B T$, for a temperature of $T = 1K$, we need to have a magnetic field of the order of 1 tesla to have

$$\frac{\mu_B B}{k_B T} \sim 1 \tag{3.5}$$

Other quantum effects that need to be included in the dynamics of the plasma are strong-field quantum electrodynamics effects. These effects become important when the plasma is subjected to ultrastrong electromagnetic fields. A more detailed description of these effects will be discussed in the next chapter.

3.2 The Wigner transformation

In the previous chapter, we used a statistical approach where the number of particles could be easily obtained by integrating the distribution function $f(\mathbf{r}, \mathbf{p}, t)$ in phase space. In quantum mechanics, the wave function can be represented either in momentum or spatial space, not both as for classical distribution functions. This makes it non-trivial to establish a statistical approach in phase space where classical interpretations can be made. However, the seminal work by Eugene Wigner [51] was a significant advance in establishing statistical approaches based on quantum formulations. The Wigner transformation, named for its inventor, has applications to different fields, including semiconductor physics, quantum optics, quantum chemistry, and plasma physics. In this thesis, we will only consider the formulation applicable to plasma physics.

The Wigner transformation can be considered as a Fourier transformation of the density matrix $\rho_{\alpha\beta}$

$$W_{\alpha\beta}(\mathbf{r}, \mathbf{p}, t) = \frac{1}{(2\pi\hbar)^3} \int d^3 z \, \langle \mathbf{r} + \mathbf{z}/2 | \, e^{\frac{i}{\hbar}\mathbf{p}\cdot\mathbf{z}} \rho_{\alpha\beta} \, | \mathbf{r} - \mathbf{z}/2 \rangle \tag{3.6}$$

where the subscripts $\alpha\beta$ here indicate the spin states. For a more detailed description of the Wigner transformation, see [52]. We can note here that the Wigner function $W_{\alpha\beta}(\mathbf{r}, \mathbf{p}, t)$ is spanned in phase space. By integrating the Wigner function in momentum space, we get

$$\int d^3 p \, W_{\alpha\beta}(\mathbf{r}, \mathbf{p}, t) = \langle \mathbf{r} | \, \rho_{\alpha\beta} \, | \mathbf{r} \rangle \tag{3.7}$$

Before considering more advanced definitions of the Wigner function, we can take a look at how one can establish kinetic equations using the Wigner

functions. As is well known, the density matrix $\rho_{\alpha\beta}$ evolves over time according to the von Neumann equation

$$i\hbar\partial_t\rho_{\alpha\beta} = \left[\hat{H}, \rho_{\alpha\beta}\right] \tag{3.8}$$

where $\hat{H}$ is the Hamiltonian. We let the Von Neumann equation be our starting point and aim to get a kinetic equation in terms of the Wigner function. Let us consider a simple case where we have a free particle with the following Hamiltonian

$$\hat{H} = \frac{p^2}{2m} \tag{3.9}$$

Using this Hamiltonian in Eq. (3.8) and making some algebraic calculations, we can obtain a kinetic equation in terms of the Wigner function

$$\left[\partial_t + \frac{\mathbf{p}}{m}\cdot\nabla_r\right] W_{\alpha\beta}(\mathbf{r},\mathbf{p},t) = 0 \tag{3.10}$$

Except for the 2×2- structure of the Wigner function [1], this equation is simply the Vlasov equation Eq. (2.4) in the vanishing field limit.

Next, we want to study the case with electromagnetic fields. Thus, we should modify the Hamiltonian to

$$\hat{H} = \frac{\left(\mathbf{p} - q\mathbf{A}(\mathbf{r})\right)^2}{2m} + q\phi(\mathbf{r}) \tag{3.11}$$

where $\mathbf{A}(\mathbf{r})$ and $\phi(\mathbf{r})$ are the vector and scalar potentials, respectively. If we use the Wigner function Eq. (3.6) for this Hamiltonian, then the kinetic equation will be explicitly dependent on the vector potential $\mathbf{A}$. This means that the kinetic equation will be gauge-dependent, and one should fix the gauge to get further when using the kinetic equation. To avoid this problem, an alternative definition of the Wigner function, which was first developed by Stratonovich [53], can be used. The idea is to use the kinetic operator

$$\boldsymbol{\pi} = \mathbf{p} - q\mathbf{A} \tag{3.12}$$

instead of the canonical operator $\hat{\mathbf{p}}$. The gauge-invariant Wigner function is now

$$W_{\alpha\beta}(\mathbf{r},\mathbf{p},t) = \frac{1}{(2\pi\hbar)^3}\int d^3z\, \langle \mathbf{r}+\mathbf{z}/2|\, e^{\frac{i}{\hbar}\mathbf{z}\cdot\left(\mathbf{p}+q\int_{1/2}^{1/2} d\lambda \mathbf{A}(\mathbf{r}+\mathbf{z}\lambda)\right)} \rho_{\alpha\beta}\, |\mathbf{r}-\mathbf{z}/2\rangle \tag{3.13}$$

[1] Since the different components of the Wigner function in Eq. (3.10) don't couple, one can easily show that this equation is reduced to a scalar-valued equation.

Because this expression is dependent on the vector potential, $\mathbf{A}$, deriving kinetic equations based on this Wigner function will be more difficult than using the gauge-dependent definition of the Wigner function Eq. (3.6). The reason is that the operators in the Hamiltonian will act on the vector potential when performing the commutator in the von Neumann equation. Nevertheless, it is necessary to obtain kinetic equations without any potential dependence. For a more detailed discussion about the technical detials related to the gauge-invariant derivation of evolution equation, see e.g., Ref. [52].

3.3 Foldy-Wouthuysen transformation

After deriving the gauge-independent Wigner function Eq. (3.13), we can now derive quantum kinetic equations of particles in external electromagnetic fields. We can let the Hamiltonian Eq. (3.11) be our starting point to derive quantum kinetic equations. However, this Hamiltonian represents non-relativistic particles in external electromagnetic fields and excludes relativistic effects. To derive quantum kinetic equations for particles under more extreme conditions, where relativistic effects are important, one needs to use another Hamiltonian. The Dirac Hamiltonian that implies the Dirac equation [54], covers relativistic effects. However, a difficulty with the Dirac Hamiltonian is that it is a 4×4 matrix where the states of matter and antimatter are coupled. While this structure is natural to deal with for problems involving the creation of electrons and positrons, i.e., when we have a strong external electric field, it is unnecessary to keep this complicated structure for modest electric fields. In Foldy and Wouthuysen's seminal paper [55], they used a transformation where one can separate the particle and antiparticle states of the Dirac Hamiltonian. Their idea was to find the non-relativistic limit of the Dirac Hamiltonian. Their starting point was the Dirac Hamiltonian

$$\hat{H} = \beta m + q\phi(\mathbf{r}) + \boldsymbol{\alpha} \cdot \hat{\boldsymbol{\pi}} \tag{3.14}$$

where β and $\boldsymbol{\alpha}$ are the Dirac matrices. The first two terms of the Dirac Hamiltonian are even since they don't couple the different states of the Dirac four-spinor. The third term is an odd term, it couples the different states of the Dirac four-spinor. The idea of Foldy and Wouthuysen was to transform the Dirac wave function, and hence the Dirac Hamiltonian, so that one only kept even terms (no coupling between the different states of the Dirac four-spinor). The Dirac wave function Ψ is then transformed according to

$$\Psi' = U\Psi \tag{3.15}$$

where $U = e^{iS}$ is a unitary operator. Here S is an operator that is assumed to have a small amplitude. The Dirac Hamiltonian is transformed according to

$$H' = U\Big(H - i\hbar\partial_t\Big)U^{-1} + i\hbar\partial_t \tag{3.16}$$

In order to get rid of the odd operators, the operator S should be defined as a product of the $\boldsymbol{\alpha}$ and β matrices. For the free particle case, we can define S as

$$S = -\frac{i}{2m}\beta\boldsymbol{\alpha}\cdot\mathbf{p}\,\omega\Big(\frac{p}{m}\Big) \tag{3.17}$$

where ω is a function of p/m determined in such a way that H' is devoid of odd operators. Using this expression of S in Eq. (3.16), we get

$$H' = \beta\Big[m\cos\left(\omega p/m\right) + p\sin\left(p/m\omega\right)\Big] + \boldsymbol{\alpha}\cdot\frac{\mathbf{p}}{p}\Big[m\cos\left(\omega p/m\right) - p\sin\left(p/m\omega\right)\Big] \tag{3.18}$$

Here, we can note that by choosing

$$\omega\Big(\frac{p}{m}\Big) = \frac{m}{p}\arctan\Big(\frac{p}{m}\Big) \tag{3.19}$$

the Hamiltonian H' becomes free of odd operators and we get

$$H' = \beta\sqrt{m^2 + p^2} \tag{3.20}$$

This Hamiltonian does not couple the upper and lower components of the Dirac four-spinor, and we got what we were looking for.

We have looked for the free particle case; next, we will look for the case of the electromagnetic field. Here, we need to consider another operator U than the one defined in Eq. (3.17). Silenko generalized the Foldy-Wouthuysen transformation to the electromagnetic case by defining the operator U [56]

$$U = \frac{\epsilon + m + \beta\boldsymbol{\alpha}\cdot\boldsymbol{\pi}}{\sqrt{2\epsilon(\epsilon + m)}} \tag{3.21}$$

where $\epsilon = \sqrt{m^2 + (\boldsymbol{\alpha}\cdot\boldsymbol{\pi})^2}$. Using this expression in Eq. (3.16), one still has odd terms. However, the odd terms are proportional to E/E_{cr}. Since we are considering a regime in which pair creation is ignored, we have $E/E_{cr} \ll 1$. Thus, the odd terms are small and can be removed by applying a second transformation, similar to the one defined in Eq. (3.16). I will skip the derivation of the second transformation since it is very lengthy, see [56] for

more details. The final Hamiltonian is obtained by considering the smallest correction of the second transformation

$$H_{FW} = \epsilon + q\phi - \frac{\mu_B m}{2}\left\{\frac{1}{\epsilon}, \boldsymbol{\sigma}\cdot\mathbf{B}\right\} + \frac{\mu_B m}{\sqrt{2\epsilon(\epsilon+m)}}\Big[\boldsymbol{\sigma}\cdot(\boldsymbol{\pi}\times\mathbf{E}) - \mathbf{E}\times\boldsymbol{\pi}\Big]\frac{1}{\sqrt{2\epsilon(\epsilon+m)}} \tag{3.22}$$

where $\boldsymbol{\sigma}$ is a vector containing the Pauli matrices. This Hamiltonian includes up to the first order of electric and magnetic field, in accordance with the $E/E_{cr} \ll 1$-approximation. Furthermore, the Hamiltonian is fully relativistic, i.e., it includes all orders of gamma-factor. This Hamiltonian has been used to derive a fully relativistic kinetic equation in [57] and in Paper I.

3.4 Ultrastrong magnetic field

In this section, we will use the Wigner function and the Foldy-Wouthuysen transformation to derive a kinetic theory of spin-1/2 particles in an ultrastrong magnetic field. When the Zeeman energy of an electron exceeds the rest mass energy, then the motion of the electron is strongly influenced by the magnetic field. Such a condition requires a magnetic field of the order of the critical one B_{cr}

$$B_{cr} = m^2/e\hbar = 4.4 \times 10^9 T \tag{3.23}$$

The Hamiltonian derived in Eq. (3.22) fulfills the conditions

$$\begin{aligned} \frac{E}{E_{cr}} &\ll 1 \\ \frac{B}{B_{cr}} &\ll 1 \end{aligned} \tag{3.24}$$

The first condition of Eq. (3.24) was used to separate the states of particles and anti-particles and to construct a simpler Hamiltonian. A strong magnetic field, on the other hand, cannot produce particles and antiparticles. Hence, it is possible to construct an even Hamiltonian, similar to Eq. (3.22), but including the effects of a strong magnetic field. To do that, we reconsider the derivation made in the previous subsection, but will not apply the approximation where we neglected the products of fields. Thus, we reconsider the Hamiltonian obtained in the previous subsection before applying the second transformation. Keeping products of fields leads to a very complicated Hamiltonian, thus we need to make a further approximation to simplify the Hamiltonian. We will consider the following division

$$\mathbf{B}(\mathbf{r}) = \mathbf{B}_0 + \delta\mathbf{B}(\mathbf{r}) \tag{3.25}$$

where we divided the magnetic field into two parts. B_0 can be considered as a background magnetic field that is homogeneous and can be very strong, i.e., $B_0 \sim B_{cr}$. The other part, δB is a varying magnetic field and fulfills the conditions of Eq. (3.24). Another approximation we will use is to neglect the effects of spin-orbit interaction, i.e., we drop the fourth term in Eq. (3.22). We do that in order to construct a less complicated kinetic equation and put more focus on the effects due to the ultra-strong magnetic fields. The final Hamiltonian is

$$\hat{H}_{FW} = \sqrt{m^2 + \pi^2 - 2m\mu_B \boldsymbol{\sigma} \cdot \mathbf{B}_0} + q\phi(\mathbf{r}) \tag{3.26}$$

Note that $\delta\mathbf{B}$ does not appear explicitly in the above Hamiltonian. However, the kinetic momentum $\hat{\boldsymbol{\pi}}$ includes the vector potential $\mathbf{A}$, which generates the full magnetic field $\mathbf{B}$. Next, we will derive a kinetic equation using this Hamiltonian. This is a similar derivation to the one made in Section 3.2 where we used the von Neumann equation Eq. (3.8). However, this time we will use the gauge-invariant Wigner function Eq. (3.13). After some algebra, we get the kinetic equation (see Paper II for more details)

$$\partial_t W_{\alpha\beta} + \frac{1}{\epsilon'}\mathbf{p} \cdot \nabla_r W_{\alpha\beta} + q\Big(\mathbf{E} + \frac{1}{\epsilon'}\mathbf{p} \times \mathbf{B}\Big) \cdot \nabla_p W_{\alpha\beta} \tag{3.27}$$

where

$$\epsilon' = \sqrt{m^2 + p^2 - 2m\mu_B \boldsymbol{\sigma} \cdot \mathbf{B}_0 - m^2\mu_B^2 (\mathbf{B}_0 \times \nabla_p)^2} \tag{3.28}$$

is the operator that generalizes the traditional Lorentz factor to include the effects of ultra-strong magnetic fields. Note that the operator ϵ' acts on everything on the right side, i.e., it acts on both $\mathbf{p}$ and $W_{\alpha\beta}$. Another thing to note is that the third term in ϵ' is matrix-valued. To obtain a scalar theory, we can make a transformation of ϵ' such that we get rid of the Pauli matrix $\boldsymbol{\sigma}$ from the square-root term. We define the scalar version of ϵ' as

$$\epsilon_\pm = \sqrt{m^2 + p^2 \mp 2m\mu_B B_0 - m^2\mu_B^2 (\mathbf{B}_0 \times \nabla_p)^2} \tag{3.29}$$

and it is straightforward to show that

$$\epsilon' = \frac{1}{2}(\epsilon_+ + \epsilon_-)I + (\epsilon_+ - \epsilon_-)\sigma_z \tag{3.30}$$

where I is the identity matrix. Note that we have assumed that $\mathbf{B}_0 = B_0\,\mathbf{e}_z$. It is worth noting that the Wigner function is a 2×2- matrix. The same is true for σ_z and I, they are also matrix-valued, but with only non-zero

diagonal elements. If the Wigner function initially has only diagonal elements, i.e., there is no coupling between the spin states

$$W_{11} = W_+, W_{22} = W_-$$
$$W_{12} = W_{21} = 0$$

Then the Wigner function remains uncoupled. Thus we can rewrite the kinetic equation Eq. (3.27) into two scalar ones

$$\partial_t W_\pm + \frac{1}{\epsilon_\pm}\mathbf{p}\cdot\nabla_r W_\pm + q\Big(\mathbf{E} + \frac{1}{\epsilon_\pm}\mathbf{p}\times\mathbf{B}\Big)\cdot\nabla_p W_\pm \tag{3.31}$$

This equation includes all orders of the spin magnetic moments. It represents an ensemble of spin-1/2 particles in the mean-field approximation in ultrastrong magnetic fields. This model could be used to model relativistic plasma that can be found around dense stars where the magnetic field exceeds the critical field B_{cr} [12]. This model is completed by Maxwell's equations

$$\nabla_r\cdot\mathbf{E} = \rho_f \tag{3.32}$$
$$\nabla_r\times\mathbf{B} = \mathbf{j}_f + \partial_t\mathbf{E} \tag{3.33}$$

where ρ_f and $\mathbf{j}_f$ are the free charge and current density respectively

$$\rho_f = q\sum_\pm \int d^3p W_\pm \tag{3.34}$$
$$\mathbf{j}_f = q\sum_\pm \int d^3p \frac{1}{\epsilon_\pm}\mathbf{p} W_\pm \tag{3.35}$$

Note that we have summed over the spin states. The model presented in this section has been derived to show that a plasma in a strong magnetic field essentially behaves as a multi-species plasma. See Paper II for more details.

Chapter 4

Pair production

In the previous chapter, we considered quantum kinetic theories, including relativistic effects and effects due to ultrastrong magnetic fields. In this section, we focus on the pair production dynamics in vacuum and plasma. Under the extreme conditions that can be found around dense stars and in the accretion discs of black holes [58], it is possible to create electrons and positrons from the vacuum. The Schwinger mechanism was presented theoretically almost a century ago, but has never been verified in experiments due to the difficulty of creating the required extreme conditions in the lab. However, with the development of laser facilities in the past decades, it is becoming more possible to observe several extreme physical phenomena (including the Schwinger mechanism) in the lab. Thus, interest in studying the Schwinger mechanism has increased over the past few decades [5, 16, 24].

The creation of electrons and positrons from vacuum becomes important when the external fields approach the critical field limit E_{cr}. At this limit, it is possible to create a large number of electrons and positrons from vacuum. The produced particles will interact with the external fields, and we will get several collective plasma effects. Thus, the focus of this chapter will be to study how the pair creation mechanism due to strong electric fields affects the dynamics of a plasma.

In this chapter, we will begin by introducing the Dirac-Heisenberg-Wigner (DHW) formalism, which is a Wigner transformation of the Dirac Hamiltonian. We will show how to define new variables in the electrostatic limit to obtain a simplified version of the DHW-formalism. Then, in Section 4.2, we will present a pair creation damping mechanism that does not rely on strong

fields but is analogous to the linear Landau-damping. To study the Schwinger effects in plasma, we solve the equations for the DHW-variables in Section 4.3. Finally, in Section 4.4, an alternative model to the DHW-formalism is presented, and the results from it are compared to the ones from the DHW-formalism.

As we have done in the previous chapter, we use units where $c = 1$.

4.1 DHW-formalism

In the previous chapter, we presented the Foldy-Wouthuysen transformation to separate the particle and antiparticle states of the Dirac Hamiltonian. However, in this section, we want to keep the coupling between the particle and anti-particle states in order to study pair production mechanisms in plasma and vacuum. Hence, the Dirac Hamiltonian Eq. (3.14) will be our starting point, and we want to derive a kinetic equation that is based on a Wigner transformation of it. In this section, I present a set of expansion coefficients, which we term the DHW-functions, of the equal-time Wigner function $W_{\alpha,\beta}(\mathbf{r},\mathbf{p},t)$ Eq. (3.13). We use the temporal gauge, where the scalar potential ϕ is set to zero, thus the electromagnetic field is given by

$$\begin{aligned}\mathbf{E} &= -\partial_t \mathbf{A}\\ \mathbf{B} &= \nabla_r \times \mathbf{A}\end{aligned}$$

The gauge-fixing slightly simplifies the derivation of the evolution equations for the DHW-functions. However, since a gauge-independent Wigner transformation is utilized, the end result will be gauge-invariant. Our starting point is the Dirac equation in the temporal gauge

$$\Big[i\hbar\partial_t + \boldsymbol{\alpha}\cdot(i\boldsymbol{\nabla}_r + q\mathbf{A}) + \beta m\Big]\hat{\Psi}_\alpha(\mathbf{r},t) = 0, \tag{4.1}$$

We use the gauge independent Wigner transformation

$$\hat{W}_{\alpha\beta}(\mathbf{r},\mathbf{p}) = \int d^3z \exp\left(-\frac{i}{\hbar}\mathbf{p}\cdot\mathbf{z} - \frac{iq}{\hbar}\int_{-1/2}^{1/2} d\lambda\, \mathbf{z}\cdot\mathbf{A}(\mathbf{r}+\lambda\mathbf{z},t)\right)\hat{C}_{\alpha\beta}(\mathbf{r},\mathbf{z},t), \tag{4.2}$$

where

$$\hat{C}_{\alpha\beta}(\mathbf{r},\mathbf{z},t) = -\frac{1}{2}\Big[\hat{\Psi}_\alpha(\mathbf{r}+\mathbf{z}/2,t), \hat{\bar{\Psi}}_\beta(\mathbf{r}-\mathbf{z}/2\Big]. \tag{4.3}$$

In Eq. (4.2) we use the Wilson line factor (the integral involving the vector potential) to ensure the gauge invariance. The Wigner function $W_{\alpha\beta}(\mathbf{r},\mathbf{p},t)$ is defined as the expectation value of the Wigner operator

$$W_{\alpha\beta}(\mathbf{r},\mathbf{p},t) = \langle\Omega|\hat{W}_{\alpha\beta}(\mathbf{r},\mathbf{p},t)|\Omega\rangle\,, \tag{4.4}$$

where $|\Omega\rangle\langle\Omega|$ is the state of the system. Note that the Wigner function Eq. (4.2) is the same as the one presented in Eq. (3.13). The only difference here is that we have expressed it in terms of the wave function Ψ instead of the density matrix ρ. Next, in order to derive an equation of motion for the Wigner function, we take the time derivative of Eq. (4.4). We use the Hartree approximation, where the electromagnetic field is treated as a non-quantized field. This approximation is well justified for high electromagnetic field strengths and amounts to neglecting the quantum fluctuations. Applying the Hartree approximation, we replace

$$\begin{aligned}\langle\Omega|\mathbf{E}(\mathbf{r},t)\hat{C}_{\alpha\beta}(\mathbf{r},\mathbf{p},t)|\Omega\rangle &\to \langle\Omega|\mathbf{E}(\mathbf{r},t)|\Omega\rangle\,\langle\Omega|\hat{C}_{\alpha\beta}(\mathbf{r},\mathbf{p},t)|\Omega\rangle\\ \langle\Omega|\mathbf{B}(\mathbf{r},t)\hat{C}_{\alpha\beta}(\mathbf{r},\mathbf{p},t)|\Omega\rangle &\to \langle\Omega|\mathbf{B}(\mathbf{r},t)|\Omega|\,\langle\Omega|\hat{C}_{\alpha\beta}(\mathbf{r},\mathbf{p},t)|\Omega\rangle\end{aligned} \tag{4.5}$$

This approximation corresponds to ignoring higher-loop radiative corrections and is appropriate for fields that vary slowly with time. After some algebra, the equation of motion of the Wigner function is given by [59]

$$i\hbar D_t W_{\alpha\beta}(\mathbf{r},\mathbf{p},t) = m[\beta,W]_{\alpha\beta} + [\tilde{\mathbf{p}}\cdot\boldsymbol{\alpha},W]_{\alpha\beta} - \frac{i\hbar}{2}\{\mathbf{D},W\}_{\alpha\beta}, \tag{4.6}$$

where we have the non-local operators

$$D_t = \frac{\partial}{\partial t} + q\tilde{\mathbf{E}}\cdot\boldsymbol{\nabla}_p \tag{4.7}$$

$$\tilde{\mathbf{p}} = \mathbf{p} - iq\int_{-1/2}^{1/2} d\tau\tau\mathbf{B}(\mathbf{r}+i\hbar\tau\boldsymbol{\nabla}_p)\times\boldsymbol{\nabla}_p \tag{4.8}$$

$$\mathbf{D} = \nabla_r + q\int_{-1/2}^{1/2} d\tau\mathbf{B}(\mathbf{r}+i\hbar\tau\boldsymbol{\nabla}_p)\times\boldsymbol{\nabla}_p \tag{4.9}$$

$$\tilde{\mathbf{E}} = \int_{-1/2}^{1/2} d\tau\mathbf{E}(\mathbf{r}+i\hbar\tau\boldsymbol{\nabla}_p) \tag{4.10}$$

which reduce to their local approximations (i.e. $D_t \to \partial/\partial t + e\mathbf{E}\cdot\nabla_p$ and $\tilde{\mathbf{E}}\to\mathbf{E}$, etc.) for scale lengths much longer than the characteristic de Broglie length.

4.1.1 The DHW-expansion

Even though the equation of motion of the Wigner function Eq. (4.6) has only a couple of terms, it is not simple to interpret since the particle and anti-particle states are mixed. The Wigner-function is a 4×4-matrix, and each component's equation of motion is coupled with others due to commutators and anti-commutators with the $\boldsymbol{\alpha}$- matrix. What is needed now is to expand the elements of the Wigner function so that it becomes possible to solve their equation of motion. We do that, by expanding the Wigner function $W(\mathbf{r}, \mathbf{p}, t)$ in terms of an irreducible set of 4×4 matrices $\{\mathbf{1}, \gamma_5, \gamma^\mu, \gamma^\mu\gamma_5, \sigma^{\mu,\nu}\}$ where $\mathbf{1}$ is a 4×4-identity matrix, we get

$$W_{\alpha\beta}(\mathbf{r}, \mathbf{p}, t) = \frac{1}{4}\Big[s + i\gamma_5\varrho + \gamma^\mu v_\mu + \gamma^\mu\gamma^5 a_\mu + \sigma^{\mu\nu}t_{\mu\nu}\Big]_{\alpha\beta}, \tag{4.11}$$

where the expansion coefficients $\{s, \varrho, v_\mu, a_\mu, t_{\mu\nu}\}$ are called the DHW-functions. This expansion leads to a number of coupled differential equations. The tensor part $\sigma^{\mu\nu}$ in Eq. (4.11) can be decomposed into

$$\mathbf{t}_1 = \begin{pmatrix} t^{10} \\ t^{20} \\ t^{30} \end{pmatrix}, \mathbf{t}_2 = \begin{pmatrix} t^{23} \\ t^{31} \\ t^{12} \end{pmatrix} \tag{4.12}$$

Using the expansion in Eq. (4.11) in Eq. (4.6), and comparing the coefficients of the basis matrices, we get the following system of partial differential equations

$$\begin{aligned}
D_t s - \frac{2}{\hbar}\tilde{\mathbf{p}} \cdot \mathbf{t}_1 &= 0 \\
D_t \varrho + \frac{2}{\hbar}\tilde{\mathbf{p}} \cdot \mathbf{t}_2 &= 2\frac{m}{\hbar}a_0 \\
D_t v_0 + \mathbf{D} \cdot \mathbf{v} &= 0 \\
D_t a_0 + \mathbf{D} \cdot \mathbf{a} &= -2\frac{m}{\hbar}\varrho \\
D_t \mathbf{v} + \mathbf{D}v_0 - \frac{2}{\hbar}\tilde{\mathbf{p}} \times \mathbf{a} &= -2\frac{m}{\hbar}\mathbf{t}_1 \\
D_t \mathbf{a} + \mathbf{D}a_0 - \frac{2}{\hbar}\tilde{\mathbf{p}} \times \mathbf{v} &= 0 \\
D_t \mathbf{t}_1 + \mathbf{D} \times \mathbf{t}_2 + \frac{2}{\hbar}\tilde{\mathbf{p}}s &= 2\frac{m}{\hbar}\mathbf{v} \\
D_t \mathbf{t}_2 - \mathbf{D} \times \mathbf{t}_1 - \frac{2}{\hbar}\tilde{\mathbf{p}}\varrho &= 0.
\end{aligned} \tag{4.13}$$

Thus we have 16 scalar components of coupled partial differential equations. This system can be expressed in matrix-form as

$$D_t \begin{pmatrix} G_1 \\ G_2 \\ G_3 \\ G_4 \end{pmatrix} = \begin{pmatrix} 0 & 0 & 0 & M_1 \\ 0 & 0 & -M_2 & 0 \\ 0 & -M_2 & 0 & -2m \\ -M_1 & 0 & 2m & 0 \end{pmatrix} \begin{pmatrix} G_1 \\ G_2 \\ G_3 \\ G_4 \end{pmatrix}, \tag{4.14}$$

where we have divided the DHW-functions into four groups

$$\begin{aligned} G_1 = \begin{pmatrix} s \\ \mathbf{t}_2 \end{pmatrix}, G_2 = \begin{pmatrix} v_0 \\ \mathbf{a} \end{pmatrix} \\ G_3 = \begin{pmatrix} a_0 \\ \mathbf{v} \end{pmatrix}, G_4 = \begin{pmatrix} \varrho \\ \mathbf{t}_1 \end{pmatrix} \end{aligned} \tag{4.15}$$

and we have defined

$$M_1 = \begin{pmatrix} \mathbf{0} & 2\tilde{\mathbf{p}} \\ 2\tilde{\mathbf{p}} & \mathbf{D}^x \end{pmatrix}, M_2 = \begin{pmatrix} \mathbf{0} & \mathbf{D} \\ \mathbf{D} & -2\tilde{\mathbf{p}}^x \end{pmatrix} \tag{4.16}$$

where $\mathbf{D}^x$ is the anti-symmetric representation of $\mathbf{D}$. One can show that some of the DHW-functions have a clear physical interpretation. Firstly, the electromagnetic current J^μ can be expressed

$$J^\mu = \frac{q}{(2\hbar\pi)^3} \int d^3p\, v^\mu(\mathbf{r}, \mathbf{p}, t) \tag{4.17}$$

where the total charge Q is

$$Q = \frac{q}{(2\hbar\pi)^2} \int d^3p d^3r v_0(\mathbf{r}, \mathbf{p}, t) \tag{4.18}$$

Moreover, the total energy W is given by

$$W = \frac{1}{(2\hbar\pi)^3} \int d^3p d^3r \big[\mathbf{p} \cdot \mathbf{v}(\mathbf{r}, \mathbf{p}, t) + ms(\mathbf{r}, \mathbf{p}.t)\big] + \frac{1}{2} \int d^3r \big[E^2 + B^2\big]. \tag{4.19}$$

The linear momentum is

$$\mathbf{p} = \frac{1}{(2\hbar\pi)^2} \int d^3p d^3r\, \mathbf{p} v_0(\mathbf{r}, \mathbf{p}, t) + \int d^3r \mathbf{E} \times \mathbf{B} \tag{4.20}$$

and the total angular momentum $\mathbf{M}$ is

$$\mathbf{M} = \frac{1}{(2\hbar\hbar\pi)^2}\int d^3p d^3r \Big[\mathbf{r}\times\mathbf{p}v_0(\mathbf{r},\mathbf{p},t) + \frac{\hbar}{2}\mathbf{a}(\mathbf{r},\mathbf{p},t)\Big] + \int d^3r\, \mathbf{r}\times\mathbf{E}\times\mathbf{B} \tag{4.21}$$

The interpretation that can be done from the expressions above is that $s(\mathbf{r},\mathbf{p},t)$ is the mass density, $v_0(\mathbf{r},\mathbf{p},t)$ is the charge density, and $\mathbf{v}(\mathbf{r},\mathbf{p},t)$ is the current density. Moreover, the function $\mathbf{a}(\mathbf{r},\mathbf{p},\mathbf{t})$ can be associated with the spin density.

The classical, but still relativistic, Vlasov equation can be obtained in the limit $\hbar \to 0$. Note, however, that the variable v_0, which is proportional to the charge density, must be kept non-zero. Thus, the procedure to reach the classical limit, which is outlined in Ref. [59], must be somewhat modified.

4.1.2 Electrostatic fields

The system in Eq. (4.13) is cumbersome to solve for the case of arbitrary geometry of external electromagnetic fields. In this section, we simplify the DHW-system Eq. (4.13) by considering one-dimensional electrostatic fields

$$\begin{aligned}\mathbf{E}(t,\mathbf{r}) &= E(t,z)\mathbf{e}_z\\ \mathbf{B}(t,\mathbf{r}) &= \mathbf{0}\end{aligned}$$

This simplifies the operators M_1 and M_2 to

$$M_1 = \begin{pmatrix}\mathbf{0} & 2\mathbf{p}\\ 2\mathbf{p} & \boldsymbol{\nabla}^x\end{pmatrix}, M_2 = \begin{pmatrix}\mathbf{0} & \boldsymbol{\nabla}_{\boldsymbol{r}}\\ \boldsymbol{\nabla}_{\boldsymbol{r}} & -2\mathbf{p}^x\end{pmatrix}. \tag{4.22}$$

By considering an electrostatic geometry, we thus get rid of some of the more complicated operators that depend on the magnetic field. However, we still have 16 coupled scalar-functions, where we will show that 8 are non-zero in the electrostatic 1D limit. However, the situation simplifies further, as only four out of the 8 nonzero DHW components are linearly independent. The problem of identifying the nonzero DHW-components as well as the smaller number of independent variables can be formulated as finding new basis vectors for the matrix system Eq. (4.14). In general, the original DHW-functions can be expressed in terms of variables $\chi_i(z,\mathbf{p},t)$, defined by

$$G(z,\mathbf{p},t) = \{G_1, G_2, G_3, G_4\} = \sum_{i=1}^{16}\chi_i(z,\mathbf{p},t)\mathbf{e}_i(z,\mathbf{p},t), \tag{4.23}$$

Here $\mathbf{e}_i(z, \mathbf{p}, t)$ are a set of orthonormal basis vectors. The idea here is to find basis vectors such that the system Eq. (4.14) reduces to equations for the linearly independent variables and reduces the number of equations to solve. The task is simplified by noting that the operator D_t will not be acting on basis vectors that depend only on $\mathbf{p}_\perp$. As a result, the problem of finding the linearly independent variables is reduced to straightforward (but somewhat tedious) linear algebra. By contracting basis vectors that only depend on $p_\perp$

$$\mathbf{e}_1 = \begin{pmatrix} 0 \\ 0 \\ \begin{pmatrix} 0 \\ \mathbf{e}_z \end{pmatrix} \\ 0 \end{pmatrix}, \ \mathbf{e}_2 = \frac{1}{\epsilon_\perp} \begin{pmatrix} \begin{pmatrix} m \\ \mathbf{0} \end{pmatrix} \\ 0 \\ \begin{pmatrix} 0 \\ \mathbf{p}_\perp \end{pmatrix} \\ 0 \end{pmatrix}$$

$$\mathbf{e}_3 = \frac{1}{\epsilon_\perp} \begin{pmatrix} 0 \\ \begin{pmatrix} 0 \\ \mathbf{e}_z \times \mathbf{p}_\perp \end{pmatrix} \\ 0 \\ \begin{pmatrix} 0 \\ -m\mathbf{e}_z \end{pmatrix} \end{pmatrix}, \ \mathbf{e}_4 = \begin{pmatrix} 0 \\ \begin{pmatrix} 1 \\ \mathbf{0} \end{pmatrix} \\ 0 \\ 0 \end{pmatrix} \tag{4.24}$$

only four independent variables $\chi_1 - \chi_4$ are needed to fully describe the system of 1D electrostatic DHW. Here $\epsilon_\perp = \sqrt{m^2 + p_\perp^2}$. Note that one only needs the basis vectors $\mathbf{e}_1 - \mathbf{e}_3$ to consider the homogeneous electrostatic case. Adding the spatial dependence into the picture makes the charge density v_0 nonzero. As a result, one extra variable and one extra basis vector $\mathbf{e}_4$ is needed, as compared to the homogeneous case considered in [60], to completely describe the system. Applying Eq. (4.23) in Eq. (4.14) for the given basis vectors, the equations in terms of $\chi_1 - \chi_4$ becomes

$$\begin{aligned} D_t\chi_1(z, \mathbf{p}, t) &= 2\epsilon_\perp(p_\perp)\chi_3(z, \mathbf{p}, t) - \frac{\partial \chi_4}{\partial z}(z, \mathbf{p}, t) \\ D_t\chi_2(z, \mathbf{p}, t) &= -2p_z\chi_3(z, \mathbf{p}, t) \\ D_t\chi_3(z, \mathbf{p}, t) &= -2\epsilon_\perp(p_\perp)\chi_1(z, \mathbf{p}, t) + 2p_z\chi_2(z, \mathbf{p}, t) \\ D_t\chi_4(z, \mathbf{p}, t) &= -\frac{\partial \chi_1}{\partial z}(z, \mathbf{p}, t) \end{aligned} \tag{4.25}$$

This system of four coupled equations is closed by Ampére's law

$$\frac{\partial E}{\partial t} = \frac{q}{(2\hbar\pi)^3} \int \chi_1 d^3p \tag{4.26}$$

where we have used the relation between the original DHW-functions and the expansion functions $\chi_i(z, \mathbf{p}, t)$. The complete list of relations between the two sets of variables is as follows:

$$\begin{aligned} s(z,\mathbf{p},t) &= \frac{m}{\epsilon_\perp}\chi_2(z,\mathbf{p},t) \\ v_0(z,\mathbf{p},t) &= \chi_4(z,\mathbf{p},t) \\ \mathbf{v}_\perp(z,\mathbf{p},t) &= \frac{\mathbf{p}_\perp}{\epsilon_\perp}\chi_2(z,\mathbf{p},t) \\ v_z(z,\mathbf{p},t) &= \chi_1(z,\mathbf{p},t) \\ a_x(z,\mathbf{p},t) &= -\frac{p_y}{\epsilon_\perp}\chi_3(z,\mathbf{p},t) \\ a_y(z,\mathbf{p},t) &= \frac{p_x}{\epsilon_\perp}\chi_3(z,\mathbf{p},t) \\ t_{1z}(z,\mathbf{p},t) &= -\frac{m}{\epsilon_\perp}\chi_3(z,\mathbf{p},t) \end{aligned} \tag{4.27}$$

As seen above, for the electrostatic case under consideration, we have 8 scalar non-zero DHW-functions. The PDE-system in Eq. (4.25) can be shown to be sufficient by using the relations between these 8 DHW-functions in the general system of Eq. (4.13).

4.1.3 Renormalization

In this subsection, we will discuss the divergence problem that appears when integrating the DHW-variables over the momentum space. Since the DHW-variables are derived from the Dirac equation, they have non-zero vacuum contributions. The vacuum contribution is present in both the mass density s and the current density $\mathbf{v}$

$$\begin{aligned} s_{\text{vac}}(\mathbf{p}) &= -\frac{2m}{\epsilon} \\ \mathbf{v}_{\text{vac}}(\mathbf{p}) &= -\frac{2\mathbf{p}}{\epsilon}, \end{aligned} \tag{4.28}$$

In terms of the χ-variables, using the relations between the DHW-variables and χ-variables in Eq. (4.27), we get

$$\begin{aligned} \chi_{1vac}(\mathbf{p}) &= -\frac{2p_z}{\epsilon} \\ \chi_{2vac}(\mathbf{p}) &= -\frac{2\epsilon_\perp}{\epsilon}. \end{aligned} \tag{4.29}$$

We will see later that these contributions will give rise to a logarithmic divergence term in the current when integrating over momentum space. To show how this problem appears and how one can treat it, we will consider the electrostatic case Eq. (4.25) for a toy model problem with only vacuum initially. Furthermore, we consider the case where we have modest electric fields such that we can linearize the DHW-variables using the ansatz

$$\chi_i(z,\mathbf{p},t) = \chi_i^0(\mathbf{p}) + \chi_i^1(\mathbf{p})e^{i(kz-\omega t)} \tag{4.30}$$

where the subscripts 0 and 1 denote the perturbed and unperturbed quantities, respectively. By using some algebra, we can find explicit expressions of the $\chi_i^1(\mathbf{p})$-variables in terms of $\chi_i^0(\mathbf{p})$, here $i = 1, 2, 3, 4$. Furthermore, by using Ampérs law Eq. (4.26), we find the dispersion relation $D(k,\omega) = 0$ of the electrostatic limit of the DHW-variables to be

$$D(k,\omega) = 1 + 4\pi e_B^2 \eta_v \tag{4.31}$$

where e_B is the bare charge and η_v is the vacuum contribution to the dispersion relation

$$\eta_v = \frac{1}{2(2\pi)^3\hbar}\int_0^\lambda d^3p \frac{1}{\epsilon^3}\left[1-\frac{p_z^2}{\epsilon^2}-\frac{\hbar^2k^2}{8\epsilon^2}\left(3-5\frac{p_z^2}{\epsilon^2}+7\frac{p_z^4}{\epsilon^4}\right)+\frac{\hbar^2\omega^2}{4\epsilon^2}\left(1-\frac{p_z^2}{\epsilon^2}\right)\right] \tag{4.32}$$

where we have introduced a momentum cut-off λ to get a finite expression. Note that we considered in Eq. (4.32) the somewhat simplified case of modest frequencies and wave-numbers, i.e., we studied the case of $\hbar\omega \ll \epsilon$ and $\hbar k \ll \epsilon$. The vacuum contribution, η_v, after integration, will give us a logarithmic divergent term and a finite term that will be the part of the vacuum polarization that remains after the renormalization.

Solving the integrals in Eq. (4.32), we get

$$\eta_v = \frac{1}{24\pi^2\hbar}\ln\left(\frac{\lambda}{m}\right) - \frac{1}{60\pi^2\hbar m^2}\left(\hbar^2k^2 - \hbar^2\omega^2\right) \tag{4.33}$$

The first term of η_v is the logarithmic term that will be absorbed by picking a proper renormalized charge e_r, and the second term is the vacuum polarization. Letting the renormalized charge e_r be given by

$$e_r^2 = \frac{e_B^2}{1+\frac{e_B^2}{24\pi^2\hbar}\ln\left(\frac{\lambda}{m}\right)} \tag{4.34}$$

Here, the logarithmic term is indeed absorbed, and the relation between e_r and e_B agrees with Ref. [61]. Next, using this expression for the renormalized charge in Eq. (4.31), we get

$$D(k,\omega) = 1 - e_r^2 \frac{\hbar^2 k^2 - \hbar^2 \omega^2}{15\pi\hbar m^2} \tag{4.35}$$

Here we have shown how the divergence problem is treated in the vacuum case. If we have the contribution from the plasma, then the dispersion relation Eq. (4.31) is extended to

$$D(k,\omega) = 1 + 4\pi\Big(e_B^2\eta_v + e_B^2\eta_p\Big) \tag{4.36}$$

where η_p is the plasma contribution to the electrostatic dispersion relation. Then, we use the same procedure where the divergence-term is absorbed in the bare charge by using Eq. (4.34) and considering modest frequencies and wave-numbers, then Eq. (4.36) becomes

$$D(k,\omega) = 1 + 4\pi e_r^2\left[\eta_p - \frac{\hbar^2 k^2 - \hbar^2 \omega^2}{60\pi^2\hbar m^2}\right] \tag{4.37}$$

The term η_p contains contributions from a real background distribution representing the plasma. Moreover, we note that the vacuum polarization term (second term in the square bracket) agrees with a general expression (proportional to derivatives of the EM-fields) for the space- and time-dependent vacuum contribution (i.e. proportional to derivatives of the EM-fields) derived in Ref. [62]. This dispersion relation will be analyzed in the following section.

4.2 One-quanta pair creation

After introducing the DHW-formalism and showing how to treat the divergence problem in the previous section, we can in this section derive a dispersion relation of the electrostatic waves in plasma, including the plasma and vacuum contributions. We will start in this section by considering the real part of the linear dispersion relation of electrostatic waves in plasma. Then, we consider a damping mechanism similar to the Landau damping. We will see that an electron-positron pair can be produced from a plasmon, and this leads to a damping of the electrostatic wave. This wave-damping mechanism is analyzed using different input parameters of the background plasma.

4.2.1 Linear dispersion relation

In Eq. (4.37), we introduced the contribution of the background plasma as η_p. Here, we will consider this contribution in more details. To do that, we go back to the step where we introduced the vacuum contribution to mass and current density (s and v). Now, a background distribution function $f_e(\mathbf{p})$ of electrons ($f_p(\mathbf{p})$ for positrons), can be added to the vacuum background (Eq. (4.28)) as follows:

$$\begin{aligned} v_0 &= 2(F+1) \\ s(\mathbf{p}) &= \frac{2m}{\epsilon} F(\mathbf{p}) \\ \mathbf{v}(\mathbf{p}) &= \frac{2\mathbf{p}}{\epsilon} F(\mathbf{p}), \end{aligned} \tag{4.38}$$

where

$$F(\mathbf{p}) = [f_p(\mathbf{p}) + f_e(\mathbf{p}) - 1] \tag{4.39}$$

represents the contribution from both the plasma and vacuum. In terms of the new functions χ_i, we have

$$\begin{aligned} \chi_1^0(\mathbf{p}) &= \frac{2p_z}{\epsilon}\Big[f_p(\mathbf{p}) + f_e(\mathbf{p}) - 1\Big] \\ \chi_2^0(\mathbf{p}) &= \frac{2\epsilon_\perp}{\epsilon}\Big[f_p(\mathbf{p}) + f_e(\mathbf{p}) - 1\Big] \\ \chi_4^0(\mathbf{p}) &= 2\Big[f_p(\mathbf{p}) - f_e(\mathbf{p})\Big] \end{aligned} \tag{4.40}$$

The electron/positron background distribution function $f_e(\mathbf{p})/f_p(\mathbf{p})$ are normalized such that the unperturbed number density $n_{0e,p}$ is

$$n_{0e,p} = \frac{2}{(2\pi\hbar)^3}\int f_{e,p}(\mathbf{p}) d^3p, \tag{4.41}$$

Without ions contributing to the charge density, we must have a neutral electron-positron background (i.e. $n_0 = n_{0e} = n_{0p}$). Adding an ion species and letting the electron and positron densities background densities differ is trivial, however. The function $f_{e,p}(\mathbf{p})$ represent an ensemble of electrons/positrons in thermodynamical equilibrium. These functions can be represented by any common background distribution function from classical kinetic theory, i.e., a Maxwell-Boltzmann, Synge-Juttner, or Fermi-Dirac distribution, depending on whether the characteristic kinetic energy is relativistic and whether the particles are degenerate. In what follows, we will

set the initial positron density to zero and consider a partially or completely degenerate Fermi-Dirac electron background f_D given by

$$f_D(\mathbf{p}) = \frac{1}{1+\exp((\epsilon-\mu)/T)}, \tag{4.42}$$

where μ is the chemical potential. Note that for a completely degenerate ($T = 0$) Fermi-Dirac background of electrons (and no positrons $f_p = 0$), the electron and vacuum contributions cancel inside the Fermi sphere. Consequently, for momenta $p \leq p_F$, where $p_F = \hbar(3\pi^2 n_0)^{1/3}$ is the Fermi momentum we have $F(\mathbf{p}) = 0$. Next, we linearize Eq. (4.25) using the plane-wave ansatz Eq. (4.30) as we did for the case with only vacuum initially in the previous section. However, this time we use Eq. (4.40) instead of Eq. (4.29). By using some algebra, we find the dispersion relation for the electrostatic wave in homogeneous plasma, including the vacuum contribution

$$D(k,\omega) = 1 + \sum_{\pm} \int \frac{d^3p}{(2\pi\hbar)^3} \frac{\pm 2e^2/(\hbar k)}{(\omega^2-k^2)(\hbar^2\omega^2 - 4p_{\pm}^2) - 4\epsilon_{\perp}^2\omega^2} \times \left[4\frac{\epsilon_{\perp}^2}{\epsilon} p_{\pm} F(\mathbf{p}) - (\hbar^2\omega^2 - 4p_{\pm}^2)\left(\frac{p_z}{\epsilon} F(\mathbf{p}) - \frac{k}{\omega} - f_D(\mathbf{p}) \right) \right] = 0 \tag{4.43}$$

where

$$p_{\pm} = p_z \pm \frac{\hbar k}{2} \tag{4.44}$$

Note that $F(\mathbf{p}) = f_D(\mathbf{p}) - 1$. Looking at the denominator of Eq. (4.43), one can see that the dispersion relation exhibits pair-creation resonances, leading to wave damping. Before studying this wave-damping mechanism, we can note that by lettering $\hbar \to 0$ in Eq. (4.43), we get

$$D(k,\omega) = 1 + \frac{e^2}{\omega} \int \frac{d^3p}{(2\pi\hbar)^3} \frac{p_z}{\epsilon} \left(\frac{1}{\omega - kp_z/\epsilon} + \frac{1}{\omega + kp_z/\epsilon} \right) \left(1 - \frac{kp_z}{\epsilon\omega} \right) \frac{\partial f_D(\mathbf{p})}{\partial p_z}. \tag{4.45}$$

We note that the appearance of $\hbar$ in the integration measure $d^3p/(2\pi\hbar)^3$ is just a matter of normalization (compare Eq. (4.41)), and not a sign of any remaining quantum features. Since f_D is an even function of p_z, it is straightforward to show that the expression Eq. (4.45) agrees with results based on the classical (but relativistic) Vlasov equation. In the next subsection, we study the wave-damping mechanism.

4.2.2 Pair creation damping

Now, we study the wave-damping mechanism that arise due to the resonance in Eq. (4.43). The calculations made in this subsection are similar to those presented in Section 2.4. With the fact that the frequency is $\omega = \omega_r + i\omega_i$ and by considering small wave-dampings $\omega_i \ll \omega_r$, we can Taylor-expand the dispersion relation Eq. (4.43) to first order around ω_r. We can then use Eq. (2.26) for the relative damping γ. What is needed to determine the relative damping γ are the real frequency ω_r and the real and imaginary parts of the dispersion relation Eq. (4.43). For ω_r and the real part of Eq. (4.43), one can note that the quantum contribution is quite small, as long as the wavenumber is modest (well beyond the Compton wavelength). This is true even for high wave frequencies, of the order of the Compton frequency or higher. Thus, unless k is very large, the relativistic Vlasov equation is a good approximation for the real part of the frequency ω_r. The reason is that for $\hbar\omega \sim mc^2$, the Fermi energy E_F will be much larger than unity. Thus, even if $\hbar\omega \sim mc^2$ we will have $\hbar\omega \ll \epsilon$, which, in turn, implies a minor quantum contribution to Eq. (4.43). Hence, when calculating the real part of the relative damping γ, we will use the relativistic Vlasov equation. However, the same conclusion does not apply for the imaginary part of the frequency, ω_i, where the full quantum relativistic theory is needed.

For simplicity, we can first consider the homogeneous case of Eq. (4.43) to determine γ. After taking the homogeneous limit of Eq. (4.43), we use spherical coordinates in momentum space and first perform the angular integration over ϕ_p and θ_p to get

$$D(k=0,\omega) = 1 + \frac{16e_B^2}{\omega^2\pi\hbar^3}\int dp \frac{p^2\epsilon}{\hbar^2\omega^2 - 4\epsilon^2}\left(1 - \frac{p^2}{3\epsilon^2}\right)\left(f - \frac{\hbar^2\omega^2}{4\epsilon^2}\right) \quad (4.46)$$

Note that we have used the bare charge e_B. However, as we will see later, the renormalization procedure is not needed for the imaginary part ω_i. In the first term of the second parentheses, we have dropped the subscript "D" on the background distribution f. The second term of the second parentheses comes from the non-zero expectation value of the vacuum contribution. To handle the denominator in Eq. (4.46), we separate the integral into the real principal value contribution and the imaginary pole contribution. The latter part will be evaluated at the resonant momenta $p = p_{res}$. Since p_{res} never approach infinity, we see that the issue of renormalization will not affect the pole contribution. Hence, for the pole contribution, one can replace the

bare charge with the real charge, i.e., $e_B \to e_r$. For the real part of the integral in Eq. (4.46), the full momentum space contributes, and hence the renormalization procedure of the previous section applies. Focusing on the pole contribution, it is convenient to factorize the denominator as follows:

$$D(k=0,\omega) = 1 + \int dp \frac{G(p)}{(\hbar\omega - 2\epsilon)(\hbar\omega + 2\epsilon)} \tag{4.47}$$

where $G(p)$ is the numerator of Eq. (4.46). Without loss of generality, we may consider only positive frequencies, in which case the pole occurs at $\epsilon(p_{res}) = \hbar\omega/2$. Changing the integration variable from p to ϵ and evaluating the integral using the Landau contour, we deduce that the imaginary part of $D(k,\omega)$ is given by

$$D_i = \frac{G(\epsilon_{res})}{4p_{res}} = -\frac{e_r^2 p_{res}}{6\pi\hbar^2\omega}\Big(1 + \frac{2m^2}{\hbar^2\omega^2}\Big)\Big(f(p_{res}) - 1\Big) \tag{4.48}$$

Now, with D_i determined, we are done with the numerator of γ Eq. (2.26). However, for the denominator of Eq. (2.26), we solve for the real frequency using the relativistic Vlasov equation in the homogeneous limit $k = 0$. Next, we can study the relative damping γ as a function of the input parameters of the background plasma. Since we are considering a Fermi-Dirac distribution of the background plasma, both the chemical potential and temperature are free parameters that the relative damping γ will depend on. We can note here, given by D_i in Eq. (4.48), in order to maximize the damping γ one should have as small $f(p_{res})$ as possible. This means that if the distribution function is more degenerate and we have a less sharp step function f, then the approximate cancellation between the vacuum and the plasma contributions is broken. A detailed analysis of the dependence of γ on temperature and chemical potential can be found in Paper IV.

For the case of general k-dependence, the dispersion relation Eq. (4.46) becomes more complicated. More specifically, the requirement for resonance will be more complicated where the resonant momentum p_{res} is modified to

$$p_{res} = \frac{1}{2}\sqrt{\frac{\hbar^2(\omega^2 - k^2) - 4m^2}{1 - \frac{k^2}{\omega^2}\cos^2\theta_p}} \tag{4.49}$$

Physically, in order to produce a pair from a plasmon, we have to fulfill the conservation of energy and momentum. When a wave quanta carries momentum $\hbar k$ in addition to energy $\hbar\omega$, electron-positron pairs with zero momentum cannot be created because the created pairs must absorb a finite

amount of momentum. As a result, a higher plasma density is required for pair-creation damping to be possible. We can deduce from this that pair creation from a plasmon is suppressed for larger wave vectors k because the pair-creation condition becomes increasingly difficult to satisfy. Paper IV contains a more detailed analysis of the k-dependence.

4.3 Plasma dynamics at the Schwinger limit

In the previous sections, we presented the DHW-formalism that covers all physics of the Dirac equation Eq. (4.1). We have analyzed the linear dispersion relation and found a damping mechanism similar to linear Landau damping. In this section, we will use the DHW-formalism to study plasma dynamics at the Schwinger limit. To do that, we can no longer make linear approximations as we have done in the previous section. Thus, we need to solve the DHW-system Eq. (4.25) numerically. To solve this PDE-system, several things need to be considered in order to simplify the numerical calculation. Firstly, we define new variables $\tilde{\chi}_i(\mathbf{p}, t)$ as the deviation from the vacuum state, i.e., we let

$$\tilde{\chi}_i(z, \mathbf{p}, t) = \chi_i(z, \mathbf{p}, t) - \chi_{i\mathrm{vac}}(\mathbf{p}). \tag{4.50}$$

where $\chi_{ivac}(\mathbf{p})$ is given by Eq. (4.29). Note that $\tilde{\chi}_3 = \chi_3$. The goal of doing this transformation is to avoid having an initial condition (vacuum contribution) that does not decay to zero at the boundaries in the momentum space. By defining the $\tilde{\chi}_i$-variables, we remove the vacuum contribution from the variables that we solve numerically. This does not mean that vacuum physics is not included in our solution, we only skip the problem of having the vacuum contribution as a part of the initial conditions. To further simplify Eq. (4.25), we consider the homogeneous limit, making the variable $\tilde{\chi}_4 = 0$. Furthermore, we introduce the so-called canonical momentum q

$$q = p_z + eA$$

By using the Canonical momentum, the operator D_t becomes

$$D_t \to \partial_t$$

Next, we normalize Eq. (4.25) using the normalized variables: $t_n = \omega_{ce} t$, $q_n = q/m$, $p_{n\perp} = p_\perp/m$, $E_n = E/E_{cr}$, $A_n = eA/m$, where $\omega_{ce} = m/\hbar$ is the Compton frequency, and we note that the χ-variables are already normalized.

For notational convenience, we omit the index n in what follows. After using all the mentioned transformations, Eq. (4.25) is now

$$\begin{aligned}
\frac{\partial \tilde{\chi}_1}{\partial t}(q, p_\perp, t) &= 2\varepsilon_\perp \tilde{\chi}_3 + 2E\frac{\varepsilon_\perp^2}{\varepsilon^3} \\
\frac{\partial \tilde{\chi}_2}{\partial t}(q, p_\perp, t) &= -2(q-A)\tilde{\chi}_3 - 2(q-A)E\frac{\varepsilon_\perp}{\varepsilon^3} \\
\frac{\partial \tilde{\chi}_3}{\partial t}(q, p_\perp, t) &= -2\varepsilon_\perp \tilde{\chi}_1 + 2(q-A)\tilde{\chi}_2
\end{aligned} \tag{4.51}$$

with Ampère's law

$$\frac{\partial E}{\partial t} = -\eta \int \chi_1 d^2p \tag{4.52}$$

where we have used the dimensionless factor $\eta = \alpha/\pi \approx 2.322 \times 10^{-3}$, here α is the fine-structure constant. Note that due to cylindrical symmetry, the azimuthal integration has already been carried out, and hence $d^2p = p_\perp dq dp_\perp$. Eq. (4.51) together with Ampere's law describe the dynamics of plasma, including the Schwinger mechanism in the mean field approximation. Generally, all quantum effects that can be described as a collective phenomenon are included in Eq. (4.51). Specifically, this includes e.g., collective pair-creation, collective pair-annihilation, Pauli-blocking, and vacuum effects such as finite vacuum polarization, see Paper VI for more details. The vacuum contribution also gives rise to the issue of charge renormalization, which has been discussed for the linear case in the previous section. However, in this section, as we solve the current integrals numerically, the divergence problem becomes less important. This is due to the use of cut-off limits in momentum space, which eliminates the divergence problem. Eqs. (4.51) and (4.52) are solved numerically using the phase corrected staggered leapfrog method [63]. While this is straightforward in principle, the full problem with three independent variables $\chi_i = \chi_i(q, p_\perp, t)$ is still numerically demanding when run on a standard workstation. The reason is that we have a strongly relativistic motion requiring a high cut-off limit in the momentum space.

4.3.1 Plasma oscillation dynamics

Now, we study the plasma oscillation dynamics by solving Eqs. (4.51) and (4.52) numerically. The initial state of the plasma is represented by the Fermi-Dirac distribution, Eq. (4.42). So by starting with a plasma initially, we can study how the different plasma parameters affect the production of electrons and positrons. Since we are considering a plasma represented by a

Fermi-Dirac distribution, we have the temperature T, the chemical potential μ and the initial field amplitude E_0 as initial parameters. A particular result from the numerical solution of Eq. (4.51)-Eq. (4.52) that we can discuss in this thesis is illustrated in Fig. 4.1, for more numerical results see Paper VI. Here the electric field and vector potential are plotted for different values of E_0, μ, and T. To be able to show the evolution of A in the same plot as E, we have normalized the vector potential once more, displaying

$$A_N = E(t=0)\frac{A(t)}{A_{\text{peak}}}$$

where A_{peak} is the peak absolute value of $A(t)$. Even in the upper panel, with a comparatively modest field strength, $E(t=0) = 1/100$, $\mu = 1$ and $T = 0.1$, we have nonlinear relativistic motion with $A_{\text{peak}} = 1.85$. In spite of the relativistic motion, the deviation from linear behavior is not clearly visible in the temporal field profile, although a careful analysis would show a harmonic content in the spectrum. However, by changing the initial electric field to $E(t=0) = 0.1$ (still with $\mu = 1$ and $T = 0.1$), the moderately relativistic motion turns into strongly relativistic oscillations with $A_{\text{peak}} = 15.9$. The oscillation is still perfectly periodic, as seen in the second panel of Fig. 1, but now there is a clear sawtooth profile of the electric field. This effect comes from the strong relativistic motion, where the gamma factors are much larger than unity for most of the oscillation, except at the turning points. As a result, for most of the oscillations, all particles move close to the speed of light, giving a current that is more or less constant until it changes direction. Given this, the sawtooth profile of the electric field is a direct consequence of Ampere's law.

Next, to be able to see quantum relativistic physics, we need to pick a stronger electric field, i.e., let $E(t=0) \sim 1$. In the third panel, we have used $E(t=0) = 1$, $\mu = 1.5$ and $T = 0.2$. Here we still see a sawtooth profile for the electric field as expected, since $A_{\text{peak}} = 67.2$. However, we now also have a pronounced decrease in the vector potential for each oscillation. While the electric field also decreases, we note that A decreases more rapidly than E. With $E = -\partial A/\partial t$ the more rapid decrease of A is consistent with an increase in the plasma frequency. While the energy loss of the electric field due to pair-production is clearly seen, the increase in plasma frequency (due to the increased number density) is even more pronounced. The latter effect is seen both in the relation between E and A, and by observing the gradual change in time period between successive peaks.

In the fourth panel, we pick $E(t=0) = 4$, $\mu = 4$ and $T = 0.2$, which

correspond to $A_{\text{peak}} = 39.7$. Here we display the dynamics of the plasma oscillation in a regime well beyond the Schwinger critical field. The curve might look surprisingly similar to the third panel with $E(1 = 0) = 1$, with the same type of energy loss and decrease in frequency. However, from the temporal scale, we see that here the oscillation frequency is much higher, due to the higher value of the electron number density. Hence the energy loss due to pair-production is indeed more rapid with a higher initial electric field, as expected.

4.3.2 Pair creation

In the previous subsection, we have seen that for fields of the order of the critical field $E \sim E_{cr}$, the plasma frequency increases due to the pair creation. This fact is further confirmed by investigating the momentum distribution of the total number of the produced pairs n. In terms of the normalized χ-variables, n can be expressed as (see Paper III for more details)

$$n = \frac{1}{(2\hbar\pi)^3} \int d^3p \frac{1}{\varepsilon} \Big[\varepsilon_\perp \tilde{\chi}_2 + (q - A)\tilde{\chi}_1 \Big] \tag{4.53}$$

The integrand in Eq. (4.53) represents the total number density, the sum of the initial plasma and the produced pairs, in momentum space. By solving the χ-variables numerically, we can follow the momentum distribution of the produced particles along with the initial plasma in the momentum space. In Fig. 4.2 contour curves over the integrand in Eq. (4.53) are shown, $n(p_\perp, p_z)$, where we have switched back to kinetic momentum p_z rather than canonical momentum q. The upper panel shows the contour curves for the initial Fermi-Dirac distribution. A quarter of a plasma period later, we can clearly distinguish the initial particle distribution. As can be seen, the initial particles have been shifted a distance $\approx A(t)$ in the p_z-direction, but with a more or less conserved shape. However, in addition to the initial plasma, a contribution from electron-positron pairs has been added, accelerated by the fields to have a much larger parallel momentum than perpendicular momentum. For a more detailed discussion about the parallel and perpendicular momentum distribution of the produced pairs, see Ref. [64]. Note that after a quarter period, the produced pairs have larger negative p_z momentum than the initial plasma. In the lower panel, after a half cycle, the symmetry has been restored, as the produced pairs are located on both sides (in parallel momentum space) of the initial plasma. As the pair-production process continues, eventually it will be difficult to separate

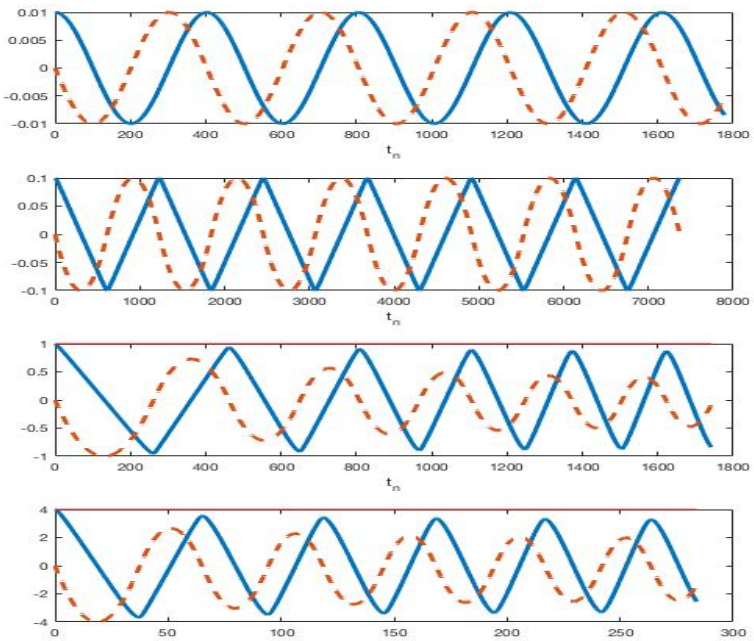

Figure 4.1: The self-consistent electric field E(t) (solid lines) and the normalized vector potential (dashed lines) are plotted over time for the initial field amplitudes $E_0 = (0.01, 0.1, 1, 4)$.

the original particles from the newly produced ones, as the produced particles will outnumber the original ones. Both Fig. 4.1 and Fig. 4.2 confirm the fact that electron-positron pairs are produced and that the wave is damped.

4.4 KGW-formalism

Until now, we have considered only the DHW-formalism to study pair production dynamics in plasma. However, the DHW-formalism is cumbersome to solve numerically for more general cases than the electrostatic one. In this section, we study the pair production dynamics in plasma using the Klein-Gordon-Wigner (KGW)-formalism [65]. This formalism is based on a Wigner transformation of the Klein-Gordon equation [66]. While the Klein-Gordon equation is used to model spinless particles, in this chapter we will show that under certain conditions the Klein-Gordon equation can be used to model pair production involving spin-1/2 particles with a sufficient accuracy..

4.4.1 A derivation of the KGW-formalism

In this subsection, we will make a brief derivation of the KGW-formalism [65]. Our starting point is the Klein-Gordon equation [66]

$$\left[(\partial_\mu - iqA_\mu)(\partial_\mu + iqA_\mu) + \frac{m^2}{\hbar^2}\right]\phi(\mathbf{r},t) = 0 \tag{4.54}$$

where $A^\mu = (A^0, \mathbf{A})$ is the vector potential in covariant form. This equation contains a second-order derivative in time. To transform the Klein-Gordon equation to phase space and obtain an explicit expression of the charge density in phase space, we express the Klein-Gordon equation in the representation of Feshbach and Villars [67]. In this representation, we have a first-order time-derivative. The Klein-Gordon field is expressed by a two-component wave function

$$\Phi = \begin{pmatrix}\psi \\ \chi\end{pmatrix} \tag{4.55}$$

where

$$\begin{aligned}\psi &= \frac{1}{2}\Big(\phi + \frac{i}{m}\frac{\partial\phi}{\partial t} - \frac{qA^0}{m}\Big) \\ \chi &= \frac{1}{2}\Big(\phi - \frac{i}{m}\frac{\partial\phi}{\partial t} + \frac{qA^0}{m}\Big)\end{aligned} \tag{4.56}$$

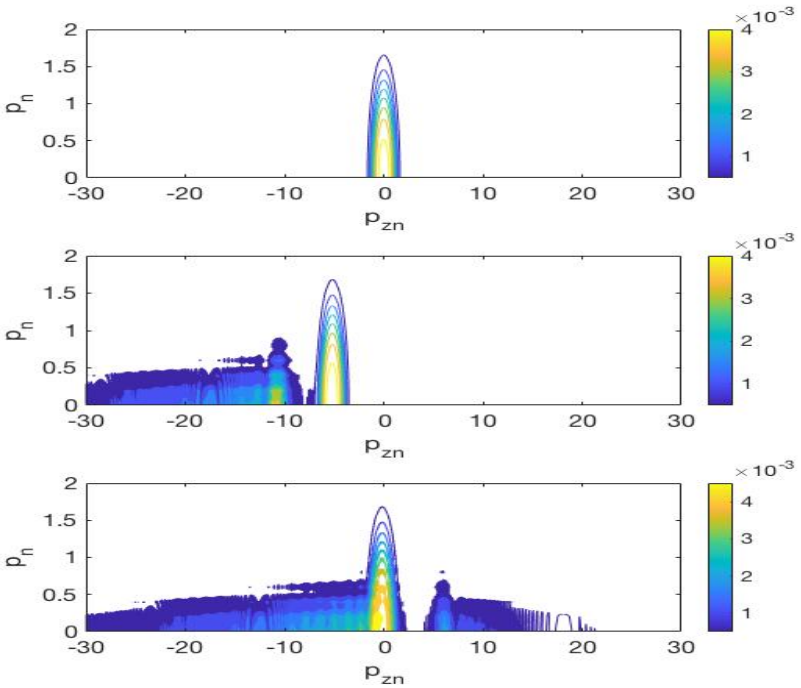

Figure 4.2: Color mappings of the momentum distribution of the total particle density $n(p_z, p_\perp)$ at three different times $t = (0, T_p/4, T_p/2)$ for $E_0 = 1$, $\mu = 1.5$ and $T = 0.2$. Here T_p is the period of the plasma oscillation.

In a matrix representation, we get

$$i\frac{\partial\Phi}{\partial t} = \left[\frac{1}{2m}\Big(-i\frac{\partial}{\partial\mathbf{r}} - q\mathbf{A}\Big)^2\begin{pmatrix}1 & 1\\ -1 & -1\end{pmatrix} + m\begin{pmatrix}1 & 0\\ 0 & -1\end{pmatrix} + qA^0\mathbf{1}\right]\Phi \quad (4.57)$$

where $\mathbf{1}$ is the identity matrix. This equation has a first-order time derivative, which means that the time evolution of the equation is of Schrödinger's type. The right-hand side of this equation can be interpreted as a Hamiltonian operator that will be used to derive a kinetic equation in phase space. Next, we use the gauge-invariant Wigner transformation Eq. (3.13). To find an evolution equation in the phase space, we take the time derivative of Eq. (3.13) and use the right-hand side of Eq. (4.57). We use the Hartree approximation, where the electromagnetic field is treated as a nonquantized field. Finally, we have an equation of motion for the Wigner function

$$\begin{aligned} i\hbar D_t W_{\alpha\beta}(\mathbf{r},\mathbf{p},t) = -\frac{i\hbar}{2}\hat{O}_1\{\sigma_3 + i\sigma_2, W\}_{\alpha\beta} \\ + \hat{O}_2[\sigma_3 + i\sigma_2, W]_{\alpha\beta} + m[\sigma_1, W]_{\alpha\beta} \end{aligned} \quad (4.58)$$

where σ_i are the Pauli matrices and we have the non-local operators

$$\begin{aligned} \hat{O}_1 &= \frac{\mathbf{p}\cdot\nabla}{m} + \frac{\mathbf{p}}{m}\cdot q\int_{1/2}^{1/2} d\lambda \mathbf{B}(\mathbf{r} + i\hbar\lambda\nabla_p)\times\nabla \\ \hat{O}_2 &= \frac{\nabla^2}{4m} - \frac{p^2}{m} - \frac{q\hbar^2}{12m}\nabla\cdot(\mathbf{B}\times\nabla) \\ &\quad + 2\frac{\mathbf{p}}{m}\cdot iq\hbar\int_{1/2}^{1/2} d\lambda \mathbf{B}(\mathbf{r} + i\hbar\lambda\nabla_p)\times\nabla_p \\ D_t &= \partial_t + q\int_{1/2}^{1/2} d\lambda \mathbf{E}(\mathbf{r} + i\hbar\lambda\nabla_p)\cdot\nabla_p \end{aligned} \quad (4.59)$$

The interpretation of Eq. (4.58) is not simple, thus we make an expansion of the Wigner function over the Pauli matrices σ_i and the identity matrix $\mathbf{1}$

$$W_{\alpha\beta}(\mathbf{r},\mathbf{p},t) = f_3(\mathbf{r},\mathbf{p},t)\mathbf{1}_{\alpha\beta} + \sum_{i=1}^{3} f_{3-i}(\mathbf{r},\mathbf{p},t)\sigma_{i,\alpha\beta} \quad (4.60)$$

where the expansion coefficients f_i, with i=0-3, will lead to four coupled partial differential equations.

$$
\begin{aligned}
D_t f_0 &= -\hat{O}_1(f_2 + f_3) \\
D_t f_1 &= -\hat{O}_2(f_2 + f_3) + 2m f_2 \\
D_t f_2 &= \hat{O}_2 f_1 + \hat{O}_1 f_0 - 2m f_1 \\
D_t f_3 &= -\hat{O}_2 f_1 - \hat{O}_1 f_0
\end{aligned}
\tag{4.61}
$$

This PDE-system is the final one that covers all physics of the Klein-Gordon equation. Compared to the DHW-formalism Eq. (4.13), this system contains only four instead of 16 scalar equations. This makes the KGW-formalism simpler to solve numerically. The 4 scalars of the KGW-formalism have a physical interpretation if one considers the following observables:

$$
\begin{aligned}
Q &= q \int d^3p d^3r\, f_0 \\
\mathbf{J} &= \frac{q}{m} \int d^3p\, \mathbf{p}(f_2 + f_3) \\
W &= \int d^3p d^3r \Big[\frac{p^2}{2m}(f_2 + f_3) + m f_3 \Big] \\
\mathbf{M} &= \int d^3p d^3r\, \mathbf{p}(f_0 - f_1)
\end{aligned}
\tag{4.62}
$$

where Q is the total charge, $\mathbf{J}$ is the total current, W is the particle energy, and $\mathbf{M}$ is the momentum. Interpretations that can be done from the above expressions include, e.g., that qf_0 is the (phase space) charge density and $q\mathbf{p}/m(f_2 + f_3)$ the current density, as implied by the sources in Maxwell's equations. The f_i-functions have the vacuum-contribution

$$
\begin{aligned}
f_0 = f_1 &= 0 \\
f_2 + f_3 &= \frac{m}{\epsilon} \\
f_3 - f_2 &= \frac{\epsilon}{m}
\end{aligned}
\tag{4.63}
$$

If we add plasma to the background, we should modify the source terms for $f_2 + f_3$ and $f_3 - f_2$. Moreover, the charge density f_0 should be non-zero. Adding electron and positron sources we first obtain $f_2 + f_3 = (m/\epsilon)F$ and $f_3 - f_2 = (\epsilon/m)F$ in Eq. (4.63) where

$$
F = 1 + 2f_e(\mathbf{p}) + 2f_p(\mathbf{p}) \tag{4.64}
$$

Here $f_{e,p}$ can be viewed as classical electron/positron distribution functions. Note that we have a positive sign between the particle and vacuum sources, instead of a negative one as in the DHW-formalism [59]. This is related to the physics of the Pauli-exclusion principle, which is not included in the KGW-formalism as the model was originally derived for spinless particles, but more directly, it comes from the sign of the vacuum expectation values. Moreover, we can note that the particle contributions to F have an extra factor of 2 in Eq. (4.64), as compared to DHW-formalism. This is due to the fact that the magnitude of the vacuum contribution is only half as large for spinless particles.

Using Eq. (4.64), the initial values of the f_i- functions due to background plasma together with the non-zero expectation value of the vacuum become

$$\begin{aligned} f_0 &= 2f_p - 2f_e \\ f_2 + f_3 &= \frac{m}{\epsilon}F \\ f_3 - f_2 &= \frac{\epsilon}{m}F \end{aligned} \tag{4.65}$$

In the next subsection, we will solve Eq. (4.61) numerically and compare the results with the ones from the DHW-formalism.

4.4.2 Numerical solution

In this subsection, we will consider the Schwinger-effects in plasma using the KGW-formalism. Before discussing the numerical solution, we can note that the process of renormalization of the KGW-formalism is done in the same way as for the DHW-formalism. Thus, we will not give more details about it in this thesis, we refer the reader who is interested to Paper VI. To be able to compare the results of the numerical solution of Eq. (4.61) with the ones from the DHW-formalism, we consider the homogeneous-limit of Eq. (4.61)

$$\begin{aligned} D_t f_0 &= 0 \\ D_t f_1 &= \frac{p^2}{m}(f_2 + f_3) + 2m f_2 \\ D_t f_2 &= -\Big(\frac{p^2}{m} + 2m\Big) f_1 \\ D_t f_3 &= \frac{p^2}{m} f_1 \end{aligned} \tag{4.66}$$

The charge density f_0 remains zero as in the DHW-formalism. In order to solve the system numerically, we need to define new variables that simplify the numerical solution. We make a new definition of the KGW-variables

$$\begin{aligned} f_1 &= f_1 \\ f_+ &= f_2 + f_3 \\ f_- &= f_2 - f_3 \end{aligned} \tag{4.67}$$

Furthermore, we redefine the KGW-variables to get rid of the initial vacuum, and we use the canonical transformation. Finally, we use normalized variables $t_n = \omega_{ce}t$, $q_n = q/m$, $p_{n\perp} = p_\perp/m$, $E_n = E/E_{cr}$, $A_n = eA/m$. Eq. (4.66) becomes now

$$\begin{aligned} \partial_t f_1 &= \epsilon^2 f_+ + f_- \\ \partial_t f_+ &= \frac{(q-A)}{\epsilon^3} E - 2f_1 \\ \partial_t f_- &= \frac{q-A}{\epsilon} E - 2\epsilon^2 f_1 \end{aligned} \tag{4.68}$$

As in the case of the DHW-formalism, the physics of the vacuum still exists in the system, we only removed the initial contribution from the KGW-variables. The Ampere's law becomes

$$\frac{\partial E}{\partial t} = -\eta \int d^2p (q-A) f_+ \tag{4.69}$$

where $\eta = \alpha/\pi$. We solve Eq. (4.68)-Eq. (4.69) numerically, neglecting the effects of the background plasma, and using the following representation of the electric field

$$E(t) = E_0 sech\Big(\frac{t}{2} - \tau_0\Big) \sin\omega t \tag{4.70}$$

where τ_0 is phase-shift and $\omega = N\omega_{ce}/100$, here N is the parameter that we vary. To check the validity of the KGW-formalism to model the dynamics of fermions, we calculate the number of produced particles in the KGW-formalism using

$$n_k = \frac{1}{(2\hbar\pi)^3} \int d^3p \frac{1}{2\epsilon} \Big[(\epsilon+1) f_+ - f_-\Big] \tag{4.71}$$

We use n_k to find the ratio n_k/n_D of the produced pair in KGW and DHW-formalism. Here n_D is the number of produced pairs in the DHW-formalism

using Eq. (4.53). For constant fields $E = E_0$, given by the rate presented for fermions in Eq. (1.2) and for bosons (same as Eq. (1.2) except factor 2 extra in the denominators), we have

$$\frac{n_k}{n_D} = \frac{1}{2} \tag{4.72}$$

For the case with a time-dependent electric field, see Fig. 4.3, we plot the ration n_k/n_D versus N. We can note that for a small N, i.e., in the constant field limit, the ratio is roughly 0.5. This is a good agreement between numerical and analytical solutions. For $N = 200$, we have $\hbar\omega = 2m$ and it is possible to create a pair from one quanta. The ratio n_k/n_D tends to be smaller than 0.5 when the one-quanta process is possible to occur. This is due to the fact that the probability of producing a pair from a single quanta is lower for KGW than for DHW; for a more detailed discussion, see Paper VII. The aim of Paper VII is to decide to what extent the simpler KGW-model can be used to describe pair production in plasma and vacuum.

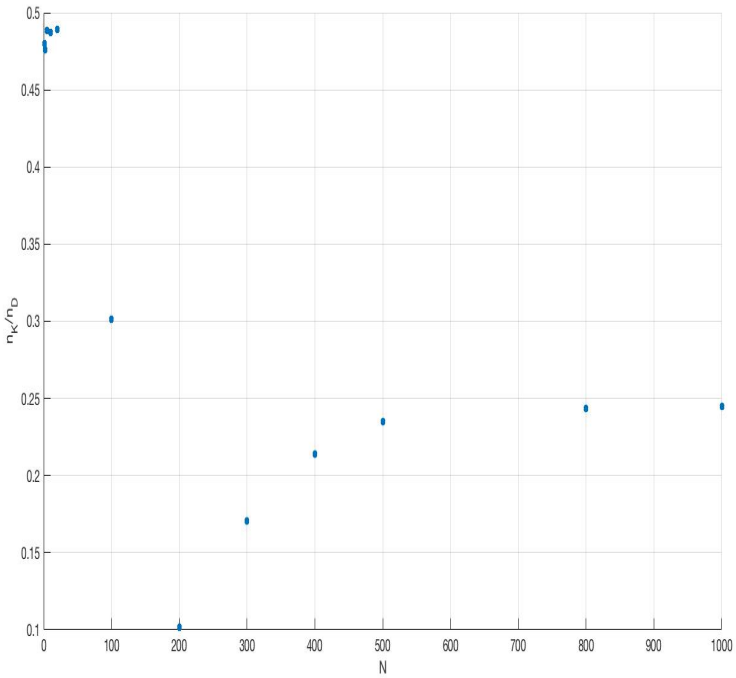

Figure 4.3: The ratio n_k/n_D is plotted as a function of N, displaying the validity of the KGW-formalism to model fermions at different frequencies of the background electric field.

Chapter 5

Radiation reaction

For sufficiently strong electromagnetic fields, the particles in the plasma emit hard photons and lose a large amount of kinetic energy. This loss of energy causes a recoil force on the emitting particles called *radiation reaction*. In the previous chapters, the focus was on including quantum effects in the kinetic description of the plasma. However, in this chapter we focus on the effects due to radiation reactions, thus we work with the classical but relativistic Vlasov equation. In particular, we study the evolution of electrostatic plasma waves, using the relativistic Vlasov equation extended by the Landau-Lifshitz expression for the radiation reaction.

We will begin this chapter by presenting the classical picture of radiation reaction physics. Then, in Section 5.2, we will show how the radiation reaction effect is added into the kinetic description of the plasma.

5.1 Classical radiation reaction

In classical electrodynamics, the motion of a charged particle in an electromagnetic field is determined by the Lorentz force $\mathbf{F}_{EM}$ [23].

$$\mathbf{F}_{EM} = q\Big(\mathbf{E} + \frac{\mathbf{p}}{c} \times \mathbf{B}\Big) \tag{5.1}$$

However, charged particles emit radiation, and in the relativistic case the emitted energy can be a substantial part of the kinetic energy. In that case, the radiation reaction force should be considered when studying the dynamics of a plasma. Classically, one can add a radiation reaction term

that corresponds to the energy loss due to radiation into the equation motion as

$$\mathbf{F} = \mathbf{F}_{EM} + \mathbf{F}_{RR} \tag{5.2}$$

Here, $\mathbf{F}$ is the total force that a particle will experience, and $\mathbf{F}_{RR}$ is the radiation reaction force. For the theory to be sound, the work performed by $\mathbf{F}_{RR}$ on the emitting particle should be the same as the radiation energy loss. The radiation reaction force $\mathbf{F}_{RR}$ can be calculated using the Lorentz-Abraham-Dirac (LAD) equation [68]. However, this equation has a problem related to the third order derivatives. This gives an unphysical solution because it is not enough to specify the initial position and momentum of the particle to solve the equation. Specifically, it can have a runaway solution, meaning that a particle can still be accelerated without external forces. This problem can be removed by using the Lorentz force F_{EM} to approximate the third-order derivative. The resulting equation is known as the Landau-Lifshitz (LL) equation and requires that

$$F_{RR} \ll F_{EM}$$

The radiation reaction force $\mathbf{F}_{RR}$ from the Landau-Lifshitz equation is

$$\begin{aligned}\mathbf{F}_{RR} = &\frac{e^3\epsilon}{6\pi\epsilon_0 m^2 c^5}\Big(\partial_t + \frac{\mathbf{p}}{\epsilon}\cdot\nabla_x\Big)\Big[\mathbf{E} + \frac{c^2\mathbf{p}}{\epsilon}\times\mathbf{B}\Big] \\ &+ \frac{e^4}{6\pi\epsilon_0 m^2 c^4}\Big[\mathbf{E}\times\mathbf{B} + \mathbf{B}\times\Big(\mathbf{B}\times\frac{c^2\mathbf{p}}{\epsilon}\Big) + \mathbf{E}\Big(\frac{c\mathbf{p}}{\epsilon}\cdot\mathbf{E}\Big)\Big] \\ &- \frac{2e^4\epsilon}{3c^7 m^4}\mathbf{p}\Big[\Big(\mathbf{E} + \frac{c^2\mathbf{p}}{\epsilon}\times\mathbf{B}\Big)^2 - \Big(\frac{c\mathbf{p}}{\epsilon}\cdot\mathbf{E}\Big)^2\Big]\end{aligned} \tag{5.3}$$

where ϵ_0 is the permittivity of free space.

5.2 Radiation reaction in relativistic plasma

For field strengths well below the Schwinger critical field E_{cr}, electron-positron pair production due to the Schwinger mechanism can be neglected. However, photon emission by single electrons due to nonlinear Compton scattering may become significant in case the product χa_0^2 is not too small. Here we have introduced the quantum nonlinearity parameter χ [5] covariantly written as

$$\chi = \frac{1}{E_{cr}c}\sqrt{F^{\mu\nu}u_\nu F_{\mu\sigma}u^\sigma}$$

which is typically much smaller than unity and the laser strength

$$a_0 = eE/m\omega$$

One can interpret a_0 roughly as the relativistic gamma factor due to electron quiver velocity for large electric fields E, in which case a_0 is larger than unity. Here, ω is the wave frequency, $F^{\mu\nu}$ the electromagnetic field tensor, and u^μ the four-velocity. Thus, for relativistic plasma motion such as $a_0 \gg 1$ and fields $E \ll E_{cr}$, it is justified to use the relativistic Vlasov equation to model plasma while also taking the radiation reaction force into account. Given Eq. (5.3), the relativistic Vlasov equation, with the radiation reaction $\mathbf{F}_{RR}$ as a correction to the Lorentz-force, can be written

$$\Big[\frac{\partial}{\partial t} + \frac{\mathbf{p}}{\epsilon}\cdot\nabla\Big]f + e\Big(\mathbf{E} + \frac{c\mathbf{p}}{\epsilon}\times\mathbf{B}\Big)\cdot\nabla_p f + \nabla_p\cdot(\mathbf{F}_{RR}f) = 0 \tag{5.4}$$

Note here that particle conservation demands the correction term to be written as $\nabla_p\cdot(\mathbf{F}_{RR}f)$ rather than $\mathbf{F}_{RR}\cdot\nabla_p f$, since, contrary to non-dissipative forces such as the Lorentz force, $\nabla_p\cdot\mathbf{F}_{RR} \neq 0$. It should be stressed that after introducing the radiation reaction into the Vlasov equation, the Maxwell-Vlasov system will not be energy-conserving anymore. This is because the macroscopic current $-e\int \mathbf{p}f/\epsilon d^3p$ will not resolve the microscopic currents from individual particles, leading to the emission of high-frequency Larmor radiation, constituting the missing piece in the energy balance.

5.2.1 Electrostatic limit

From now on we will consider the one-dimensional electrostatic limit with $\mathbf{E} = E(z,t)\hat{\mathbf{z}}$, in which case the radiation reaction force Eq. (5.3) reduces to

$$\mathbf{F}_{RR} = \frac{e^3\epsilon}{6\pi\epsilon_0 m^2c^5}\Big[\Big(\frac{\partial E}{\partial t} + \frac{p_z}{\epsilon}\frac{\partial E}{\partial z}\Big)\mathbf{e}_z + \frac{c^2eE^2p_z}{\epsilon^2}\mathbf{e}_z - \frac{eE^2\epsilon_\perp^2}{m^2c^2\epsilon^2}\mathbf{p}\Big] \tag{5.5}$$

As a consequence, in the electrostatic 1D limit, the relativistic Vlasov equation including radiation reactions is given by

$$\Big(\frac{\partial}{\partial t_n} + \frac{p_{zn}}{\epsilon_n}\frac{\partial}{\partial z_n} + E_n\frac{\partial}{\partial p_{zn}}\Big)f_n - \frac{1}{p_{\perp n}}\frac{\partial}{\partial p_{\perp n}}\Big(\frac{2\delta\epsilon_{\perp n}^2p_{\perp n}^2E_n^2}{3\epsilon_n}f_n\Big) + \frac{2\delta}{3}\frac{\partial}{\partial p_{zn}}\Big[\Big(\epsilon_n\frac{\partial E_n}{\partial t_n} + p_{zn}\frac{\partial E_n}{\partial z_n} - \frac{E_n^2p_{zn}p_{\perp n}^2}{\epsilon_n}\Big)f_n\Big] = 0 \tag{5.6}$$

where we have used normalized units

$$\begin{aligned} t_n &= \omega_p t \\ z_n &= \frac{\omega_p z}{c} \\ p_n &= \frac{p}{mc} \\ \epsilon_n &= \frac{\epsilon}{mc^2} \\ f_n &= \frac{m^3 c^3}{n_0} f \\ E_n &= \frac{eE}{mc\omega_p} \end{aligned} \tag{5.7}$$

Here $\delta = r_e \omega_p / c$ and r_e is the classical electron radius, that is $r_e = e^2/mc^2$. We note that except for extremely high-density plasmas (like, for example, the central parts of neutron stars), $\delta \ll 1$ applies, which will be used for the reminder of this section. Finally, the radiation reaction corrected Vlasov Eq. (5.6), is complemented by Ampère's law to obtain a closed system.

$$\frac{\partial E_n}{\partial t_n} = -\int d^3 p_n \frac{p_{zn}}{\epsilon_n} f_n \tag{5.8}$$

5.2.2 Plasma cooling

We solve Eq. (5.6) and Eq. (5.8) numerically in the homogeneous limit. Generally, the radiation reaction force leads to a damping of the plasma oscillation. In this subsection, we focus on the effect of the radiation reaction force on the background plasma, for more details about the plasma oscillation damping, see Paper V. As our initial background distribution, we will consider a Maxwell-Jüttner distribution f_0, i.e., we let

$$f_0 = \frac{1}{\int e^{-\sqrt{1+p_\perp^2+q^2}/E_{th}} p_\perp dp_\perp dq} e^{-\sqrt{1+p_\perp^2+q^2}/E_{th}} \tag{5.9}$$

where we have used the canonical momentum q to simplify the numerical calculation as we have done in the previous chapters, and p_{th} is the normalized thermal momentum. We have used the thermal energy

$$E_{th} = \sqrt{1+p_{th}^2} - 1$$

Since we have $\delta \ll 1$, the radiation reaction term in Eq. (5.6) will be a small correction to the relativistic Vlasov equation. Thus, we define

$$f = f_v + \delta f$$

where f_v is a solution to the unperturbed Vlasov equation (i.e. for $\delta = 0$ in Eq. (5.6)) and δf is due to the radiation reaction. Next, we can define temperature $T = T_0 + \delta T$, where T_0 is the (constant) initial temperature of the background plasma, and the temperature change δT is given by

$$\delta T = \frac{2}{3} \int \left[\sqrt{1 + q^2 + p_\perp^2} - 1 \right] \delta f p_\perp dp_\perp dq \tag{5.10}$$

together with

$$\delta f = \int_0^t -\nabla_{\tilde{p}} \cdot \Big(\mathbf{F}_{rad}\, f_v(q, p_\perp, t = 0) \Big) dt' \tag{5.11}$$

Inserting the expression for Eq. (5.11) into Eq. (5.10), after a partial integration we can derive an expression for δT

$$\delta T = \frac{4\delta}{6} \int p_\perp dp_\perp dq \left(q \frac{\partial E}{\partial t} - \frac{(1 + p_\perp^2 + q^2 - qA)}{\epsilon^2} E^2 p_\perp^2 \right) \frac{\epsilon}{\epsilon_q} f_v \tag{5.12}$$

where

$$\begin{aligned} \epsilon &= \sqrt{1 + p_\perp^2 + (q - A)^2} \\ \epsilon_q &= \sqrt{1 + p_\perp^2 + q^2} \end{aligned} \tag{5.13}$$

So the change in the temperature of the plasma δT is obtained by solving the unperturbed Vlasov Eq. (5.6), then using Eq. (5.12). In Fig. 5.1, we present the result of the numerical solution of δT Eq. (5.12). In the upper panel of Fig. 5.1 the evolution of the normalized temperature $T_{rel} = (T_0 + \delta T)/T_0$ is displayed for the initial electric field $E_0 = 3$ and $\delta = 0.01$ for different initial temperatures. We can see that the relative temperature decrease is only somewhat stronger at higher temperatures. While the relative difference in the cooling rate due to the difference in initial thermal energy is fairly modest, in absolute terms, the cooling is naturally much more pronounced for a higher initial temperature. In the lower panel of Fig. 5.1, the evolution of the normalized temperature T_{rel} is shown for different values of the initial electric field, E_0, for $p_{th} = 0.1$. As is obvious, the cooling rate shows a very strong dependence on the initial electric field. Roughly speaking, the temperature loss rate is proportional to E_0^2, as can be expected from Eq. (5.12).

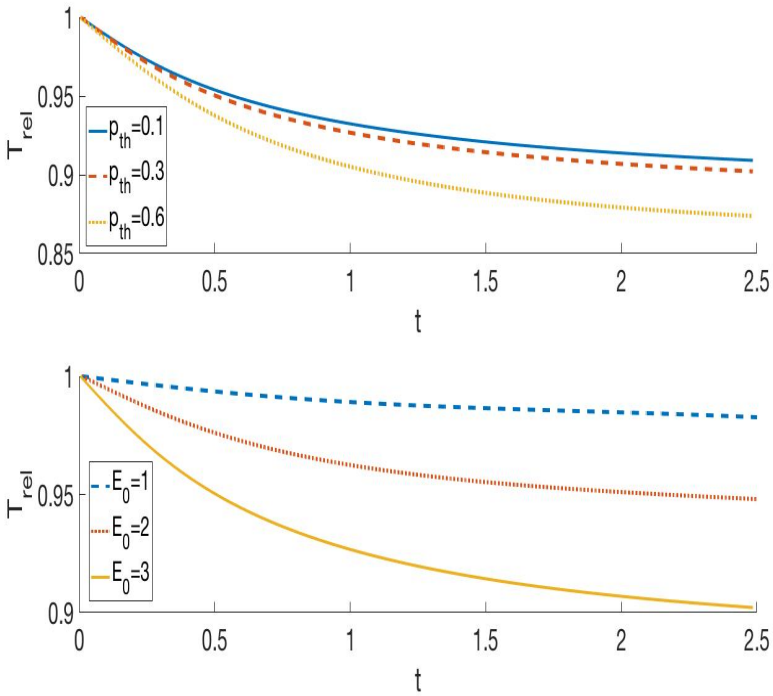

Figure 5.1: T_{rel} as a function of time t. In the first panel we have $E_0 = 3$, $\delta = 0.01$ and $p_{th} = (0.1, 0.3, 0.5)$. In the second panel we have $p_{th} = 0.3$, $\delta = 0.01$ and $E_0 = (1, 2, 3)$.

Summary of Papers

Paper I
Relativistic kinetic theory for spin-1/2 particles: Conservation laws, thermodynamics, and linear waves
In this paper, we have studied a fully relativistic quantum kinetic equation for spin-1/2 particles. We have derived a full set of conservation laws, including those governing momentum, energy, and angular momentum. Furthermore, we addressed thermodynamical background functions for different cases. These have been used to calculate the linear dispersion of waves in plasma.
My contribution to this work was to derive linear dispersion relations for waves propagating in magnetized plasma. I also took part in writing a large part of the report.

Paper II
Kinetic theory for spin-1/2 particles in ultrastrong magnetic fields
In this work, we developed a fully relativistic quantum kinetic theory for spin-1/2 particles in ultrastrong magnetic fields. The kinetic equation is derived using a Foldy-Wouthuysen transformation of the Dirac Hamiltonian, where the particle and antiparticle states are decoupled. Then, we applied a Wigner transformation to the new Hamiltonian, and the kinetic theory was derived.
My contribution to this paper included making the transformation, deriving the kinetic equation, and calculating the linear dispersion relations. I have been doing the majority of the calculations and writing a large part of the report. I also took part in analyzing the results of the calculations.

Paper III
Plasma dynamics and vacuum pair creation using the Dirac-Heisenberg-Wigner formalism

In this work, we derived a system of coupled partial differential equations for the equal-time Wigner function in an arbitrary strong electromagnetic field. We started the paper by presenting the Dirac-Heisenberg-Wigner formalism. Then, we presented a system of four coupled partial differential equations in the electrostatic limit. This system enables the numerical study of the plasma dynamics at the Schwinger limit. This electrostatic system was further studied in two different cases. In the first case, we considered linearized wave propagation in a plasma, accounting for the nonzero vacuum expectation values. In the second case, we considered Schwinger pair production using the local density approximation to allow for analytical treatment.
My contribution to this paper included deriving the electrostatic system, calculating the linear dispersion relation, and making the calculation of the local density approximation. I have been doing the majority of the calculations and writing a large part of the report. I also took part in analyzing the results of the calculations.

Paper IV
Linear pair-creation damping of high-frequency plasma oscillation
In this work, we have studied the linear dispersion relation for Langmuir waves in plasmas of very high density, based on the Dirac–Heisenberg–Wigner formalism. This work was based on the electrostatic system derived in Paper III. We have discussed ultraviolet divergences that appear due to the vacuum contribution to the physical observables. We have removed the ultraviolet divergences by charge renormalization and shown that the remaining vacuum contribution agrees with previously derived expressions. The main new feature of this work was a damping mechanism similar to Landau damping, but where the plasmon energy gives rise to the creation of electron–positron pairs. Finally, the analytical results of linearized theory were compared with numerical solutions.
My contribution to this paper included the derivation of the linear dispersion relation, calculating the charge renormalization, and constructing the numerical solutions. I have been doing the majority of the calculations and writing a large part of the report. I also took part in analyzing the results of the calculations.

Paper V
Radiation reaction effects in relativistic plasmas–the electrostatic limit
In this work, we have studied the evolution of electrostatic plasma waves using

the relativistic Vlasov equation extended by the Landau-Lifshitz radiation reaction. We solved the system numerically and calculated the Langmuir wave damping as a function of wave number, initial temperature, and initial electric field amplitude. Moreover, we found that the background distribution function loses energy in the process. Then, we calculated the cooling rate as a function of the initial temperature and the initial wave amplitude.
My contribution to this paper included constructing the numerical solutions of the equations studied in this work. I have been writing a large part of the report. I also took part in analyzing the results of the calculations.

Paper VI
Plasma dynamics at the Schwinger limit and beyond
In this work, we used the Dirac-Heisenberg-Wigner formalism to study the interplay between classical and quantum mechanical mechanisms in the regime of ultrastrong electric fields. This work was based on the electrostatic system derived in Paper III. In particular, we studied the effects of initial density and temperature on the plasma oscillation dynamics. Finally, comparisons with competing mechanisms such as radiation reaction and Breit-Wheeler pair production were made.
My contribution to this paper included taking part in constructing the numerical solutions. I also took part in analyzing the results of the calculations and writing the report.

Paper VII
Applicability of the Klein-Gordon equation for pair production in vacuum and plasma
In this work, we have studied pair production mechanisms in plasma and vacuum using a model based on the Wigner transformation of the Klein-Gordon equation. We started the work by presenting the model and deriving a linear dispersion relation for electromagnetic waves. Then, the Klein-Gordon model was solved numerically in the electrostatic limit. Both the numerical and analytical results were analyzed and compared with the Dirac-Heisenberg-Wigner model.
My contribution to this paper included constructing the numerical solutions of the Klein-Gordon model and deriving the linear dispersion relation. I have been writing a large part of the report. I also took part in analyzing the results of the calculations.

Acknowledgements

First of all, I would like to thank my supervisor, Gert Brodin, for believing in me and supporting me during my time as a Ph.D. student. You have been generous with your time, guidance, and support.

I would also like to thank Jens Zamanian and Greger Torgrimsson for the helpful discussions. Jens, thank you for helping me design the cover of the thesis. Greger, I really appreciated the discussions I had with you about the different issues related to the QED extensions of the plasma models. Thanks also to Robin Ekman for all the discussions we had during my entire Ph.D. time.

There are many people that I would like to thank, including Michael Bradley. You have been very generous with your time, and I enjoyed the time we spent teaching together. Thank you also to Philip; best of luck and keep up the good work during the rest of your Ph.D. To László Veisz, thank you for the discussions we had about experimental physics. Finally, I would like to thank Thomas Wågberg for all his administrative help during my Ph.D. time.

Outside the department, I would like to thank Bengt Eliasson for all the discussions we had about numerical analysis. To Christian Kohlfürst, thank you for the discussions we had about the DHW-formalism. I would like to thank Mattias Marklund for supervising my Master's thesis and the discussion we had during my Ph.D. Thanks also to Frederico Fiuza and David Reis at Stanford University for all the discussions and guidance during my Ph.D.

Finally, I thank my family for their support. Without you, I would not be able to write this thesis.

Bibliography

[1] H. Abramowicz et al., "Conceptual design report for the luxe experiment", The European Physical Journal Special Topics **230**, 2445–2560 (2021).

[2] A. Matheron et al., "Probing strong-field qed in beam-plasma collisions", arXiv preprint arXiv:2209.14280 (2022).

[3] C. N. Danson et al., "Petawatt and exawatt class lasers worldwide", High Power Laser Science and Engineering **7**, e54 (2019).

[4] E. Cartlidge, *The light fantastic*, 2018.

[5] A. Fedotov et al., "Advances in qed with intense background fields", Physics Reports **1010**, 1–138 (2023).

[6] A. Di Piazza, C. Müller, and K. Hatsagortsyan, "Extremely high-intensity laser interactions with fundamental quantum systems", Reviews of Modern Physics **84**, 1177 (2012).

[7] A. Gonoskov et al., "Extended particle-in-cell schemes for physics in ultrastrong laser fields: review and developments", Phys. Rev. E **92**, 023305 (2015).

[8] J. Mendonca, *Theory of photon acceleration* (CRC Press, 2000).

[9] J. Vieira and J. T. Mendonca, "Nonlinear laser driven donut wakefields for positron and electron acceleration", Phys. Rev. Lett. **112**, 215001 (2014).

[10] A. Gonoskov et al., "Probing nonperturbative qed with optimally focused laser pulses", Phys. Rev. Lett. **111**, 060404 (2013).

[11] M. J. A. Jansen et al., "Strong-field breit-wheeler pair production in short laser pulses: relevance of spin effects", Phys. Rev. D **94**, 013010 (2016).

[12] D. A. Uzdensky and S. Rightley, "Plasma physics of extreme astrophysical environments", Reports on Progress in Physics **77**, 036902 (2014).

[13] F. Sauter, "Über das verhalten eines elektrons im homogenen elektrischen feld nach der relativistischen theorie diracs", Zeitschrift für Physik **69**, 742–764 (1931).

[14] J. Schwinger, "On gauge invariance and vacuum polarization", Phys. Rev. **82**, 664–679 (1951).

[15] F. Hebenstreit, R. Alkofer, and H. Gies, "Schwinger pair production in space- and time-dependent electric fields: relating the wigner formalism to quantum kinetic theory", Phys. Rev. D **82**, 105026 (2010).

[16] G. Torgrimsson, C. Schneider, and R. Schützhold, "Sauter-schwinger pair creation dynamically assisted by a plane wave", Phys. Rev. D **97**, 096004 (2018).

[17] C. Kohlfürst et al., "Optimizing the pulse shape for schwinger pair production", Phys. Rev. D **88**, 045028 (2013).

[18] G. Breit and J. A. Wheeler, "Collision of two light quanta", Phys. Rev. **46**, 1087–1091 (1934).

[19] D. L. Burke et al., "Positron production in multiphoton light-by-light scattering", Phys. Rev. Lett. **79**, 1626–1629 (1997).

[20] M. Abraham, "Theorie der elektrizität, ii, teubner", Leipzig (1905, 1923) (1905).

[21] H. A. Lorentz, *The theory of electrons and its applications to the phenomena of light and radiant heat*, Vol. 29 (GE Stechert & Company, 1916).

[22] L. D. Landau and E. M. Lifshitz, *Statistical physics: volume 5*, Vol. 5 (Elsevier, 2013).

[23] J. D. Jackson, "Classical electrodynamics 3rd ed john wiley & sons", Inc., NewYork, NY (1999).

[24] G. Torgrimsson, *Pair production, vacuum birefringence and radiation reaction in strong field qed* (Chalmers Tekniska Hogskola (Sweden), 2016).

[25] A. Gonoskov et al., "Charged particle motion and radiation in strong electromagnetic fields", Rev. Mod. Phys. **94**, 045001 (2022).

[26] T. G. Blackburn et al., "Benchmarking semiclassical approaches to strong-field qed: nonlinear compton scattering in intense laser pulses", Physics of Plasmas **25**, 083108 (2018).

[27] N. Neitz and A. Di Piazza, "Stochasticity effects in quantum radiation reaction", Phys. Rev. Lett. **111**, 054802 (2013).

[28] J. M. Cole et al., "Experimental evidence of radiation reaction in the collision of a high-intensity laser pulse with a laser-wakefield accelerated electron beam", Phys. Rev. X **8**, 011020 (2018).

[29] D. Del Sorbo et al., "Spin polarization of electrons by ultraintense lasers", Phys. Rev. A **96**, 043407 (2017).

[30] W. Heisenberg and H. Euler, "Folgerungen aus der diracschen theorie des positrons", Zeitschrift für Physik **98**, 714–732 (1936).

[31] W. Dittrich and H. Gies, *Probing the quantum vacuum: perturbative effective action approach in quantum electrodynamics and its application*, Vol. 166 (Springer Science & Business Media, 2000).

[32] S. L. Adler, "Photon splitting and photon dispersion in a strong magnetic field", Annals of Physics **67**, 599–647 (1971).

[33] G. Aad et al., "Observation of light-by-light scattering in ultraperipheral pb+ pb collisions with the atlas detector", Physical review letters **123**, 052001 (2019).

[34] D. R. Nicholson and D. R. Nicholson, *Introduction to plasma theory*, Vol. 1 (Wiley New York, 1983).

[35] R. O. Dendy, *Plasma physics: an introductory course* (Cambridge University Press, 1995).

[36] I. Langmuir, "Oscillations in ionized gases", Proceedings of the National Academy of Sciences **14**, 627–637 (1928).

[37] P. Debye and E. Hückel, "De la theorie des electrolytes. i. abaissement du point de congelation et phenomenes associes", Physikalische Zeitschrift **24**, 185–206 (1923).

[38] A. Vlasov, "Theory of vibrational properties of electron gas and its applications", Uch. Rec. MSU (1945).

[39] L. Landau, "On the vibrations of the electronic plasma (collected papers)", Gorden and Breach, New York, 445–460 (1946).

[40] G. Castro et al., "Comparison between off-resonance and electron bernstein waves heating regime in a microwave discharge ion source", Review of Scientific Instruments **83**, 02B501 (2012).

[41] N. A. Krall and A. W. Trivelpiece, "Principles of plasma physics", American Journal of Physics **41**, 1380–1381 (1973).

[42] G. Brodin and J. Zamanian, "Quantum kinetic theory of plasmas", Reviews of Modern Plasma Physics **6**, 4 (2022).

[43] D. Melrose, "Quantum kinetic theory for unmagnetized and magnetized plasmas: a tutorial review of quantum plasma theory", Reviews of Modern Plasma Physics **4**, 8 (2020).

[44] S. Glenzer et al., "Observations of plasmons in warm dense matter", Physical review letters **98**, 065002 (2007).

[45] H. Lee et al., "X-ray thomson-scattering measurements of density and temperature in shock-compressed beryllium", Physical review letters **102**, 115001 (2009).

[46] S. Wolf et al., "Spintronics: a spin-based electronics vision for the future", science **294**, 1488–1495 (2001).

[47] I. Žutić, J. Fabian, and S. D. Sarma, "Spintronics: fundamentals and applications", Reviews of modern physics **76**, 323 (2004).

[48] E. Ozbay, "Plasmonics: merging photonics and electronics at nanoscale dimensions", science **311**, 189–193 (2006).

[49] M. Marklund et al., "New quantum limits in plasmonic devices", Europhysics letters **84**, 17006 (2008).

[50] J. Pitarke et al., "Theory of surface plasmons and surface-plasmon polaritons", Reports on progress in physics **70**, 1 (2006).

[51] E. P. Wigner, "On the quantum correction for thermodynamic equilibrium", in *Part i: physical chemistry. part ii: solid state physics* (Springer, 1997), pp. 110–120.

[52] J. Zamanian, M. Marklund, and G. Brodin, "Scalar quantum kinetic theory for spin-1/2 particles: mean field theory", New Journal of Physics **12**, 043019 (2010).

[53] R. Stratonovich, "Gauge invariant generalization of wigner distribution", Doklady Akademii Nauk SSSR **109**, 72–75 (1956).

[54] P. A. M. Dirac, "The quantum theory of the electron", Proceedings of the Royal Society of London. Series A, Containing Papers of a Mathematical and Physical Character **117**, 610–624 (1928).

[55] L. L. Foldy and S. A. Wouthuysen, "On the dirac theory of spin 1/2 particles and its non-relativistic limit", Phys. Rev. **78**, 29–36 (1950).

[56] A. J. Silenko, "Foldy-wouthyusen transformation and semiclassical limit for relativistic particles in strong external fields", Phys. Rev. A **77**, 012116 (2008).

[57] R. Ekman, F. A. Asenjo, and J. Zamanian, "Relativistic kinetic equation for spin-1/2 particles in the long-scale-length approximation", Phys. Rev. E **96**, 023207 (2017).

[58] D. A. Uzdensky and S. Rightley, "Plasma physics of extreme astrophysical environments", Rep. Prog. Phys. **77**, 036902 (2014).

[59] I. Bialynicki-Birula, P. Górnicki, and J. Rafelski, "Phase-space structure of the dirac vacuum", Phys. Rev. D **44**, 1825–1835 (1991).

[60] X.-l. Sheng et al., "Wigner function and pair production in parallel electric and magnetic fields", Phys. Rev. D **99**, 056004 (2019).

[61] J. C. R. Bloch et al., "Pair creation: back reactions and damping", Phys. Rev. D **60**, 116011 (1999).

[62] S. Mamayev, V. Mostepanenko, and M. Eides, "Effective action for a non-stationary electromagnetic field", Sov. J. Nucl. Phys.(Engl. Transl.);(United States) **33** (1981).

[63] W. H. Press et al., *Numerical recipes 3rd edition: the art of scientific computing* (Cambridge university press, 2007).

[64] K. Krajewska and J. Z. Kami ński, "Threshold effects in electron-positron pair creation from the vacuum: stabilization and longitudinal versus transverse momentum sharing", Phys. Rev. A **100**, 012104 (2019).

[65] C. Best, P. Gornicki, and W. Greiner, "The phase-space structure of the klein-gordon field", Annals of Physics **225**, 169–190 (1993).

[66] W. Gordon, "Der comptoneffekt nach der schrödingerschen theorie", Zeitschrift für Physik **40**, 117–133 (1926).

[67] H. Feshbach and F. Villars, "Elementary relativistic wave mechanics of spin 0 and spin 1/2 particles", Reviews of Modern Physics **30**, 24 (1958).

[68] P. A. M. Dirac, "Classical theory of radiating electrons", Proceedings of the Royal Society of London. Series A. Mathematical and Physical Sciences **167**, 148–169 (1938).